Atmospheric
Chemistry
and Physics
Discussions

Open Access

An overview of regional and local characteristics of aerosols in South Africa using satellite, ground, and modeling data

S. P. Hersey[1], R. M. Garland[1,2], E. Crosbie[3], T. Shingler[3], A. Sorooshian[3,4], S. Piketh[1], and R. Burger[1]

[1]Department of Environmental Sciences and Management, North-West University, Potchefstroom, South Africa
[2]Council for Scientific and Industrial Research (CSIR), Pretoria, South Africa
[3]Department of Atmospheric Sciences, University of Arizona, Tucson, AZ, USA
[4]Department of Chemical and Environmental Engineering, University of Arizona, Tucson, AZ, USA

Correspondence to: S. P. Hersey (scott.hersey@gmail.com)

Discussion Paper | Discussion Paper | Discussion Paper | Discussion Paper

Title Page

Abstract	Introduction
Conclusions	References
Tables	Figures

|◄ | ►|
◄ | ►

Back | Close

Full Screen / Esc

Printer-friendly Version

Interactive Discussion

South African aerosol

S. P. Hersey et al.

Title Page

Abstract	Introduction
Conclusions	References
Tables	Figures

|◀ | ▶|

◀ | ▶

Back | Close

Full Screen / Esc

Printer-friendly Version

Interactive Discussion

Abstract

We present a comprehensive overview of particulate air quality across the five major metropolitan areas of South Africa (Cape Town, Bloemfontein, Johannesburg and Tshwane (Gauteng Province), the Industrial Highveld Air Quality Priority Area (HVAPA), and Durban), based on a decadal (1 January 2000 to 31 December 2009) aerosol climatology from multiple satellite platforms and a detailed analysis of ground-based data from 19 sites throughout Gauteng. Data include Aerosol Optical Depth ($AOD_{550,555}$) from Aqua (550 nm), Terra (550 nm), and MISR (555 nm) platforms, Ängström Exponent ($\alpha_{550/865,470/660}$) from Aqua (550/865 nm) and Terra (470/660 nm), Ultraviolet Aerosol Index (UVAI) from TOMS, and model results from the Goddard Ozone Chemistry Aerosol Radiation and Transport (GOCART) model. Results in Cape Town are distinct, owing to a typically clean, marine airmass origin and infrequent continental influence. At continentally-influenced sites, AOD_{550}, AOD_{555}, $\alpha_{550/865}$, $\alpha_{470/660}$ and UVAI reach maxima (0.12–0.20, 1.0–1.8, and 1.0–1.2, respectively) during late winter and early spring (August–October), coinciding with a period of enhanced dust generation and the maximum frequency of close-proximity and subtropical fires identified by MODIS Fire Information for Resource Management System (FIRMS). The adjacent metropolitan and industrial Gauteng and HVAPA areas have been identified as a megacity based on NO_2 concentrations, but AOD is a factor of 3–6 lower than other megacities worldwide. GOCART results suggest that the contributions of organics and black carbon to AOD are significantly enhanced during biomass burning season (ASO), but that sulfate is the most significant contributor to AOD (~ 70–80 %) through the rest of the year. Dust appears to be underestimated by GOCART emissions inventories at continentally-influenced metropolitan areas of South Africa.

Ground monitoring sites were classified according to site type: (1) township and informal settlement sites with domestic burning influence, (2) urban and suburban residential sites with no domestic burning in the immediate vicinity, (3) industrial sites, and (4) one traffic site situated at a major freeway interchange. PM_{10} concentrations in

township areas are 56 % higher than in developed residential areas and 78 % higher than in industrial areas as an annual average, with PM_{10} in townships 63 and 136 % higher than developed residential and industrial areas, respectively, in winter (June, July, August). Monthly PM_{10} and $PM_{2.5}$ concentrations reach annual maxima during winter at all sites except in industrial areas. At industrial sites, maxima in PM_{10} and $PM_{2.5}$ tend to occur during summer (December–February), when photochemical generation of secondary aerosol is expected and when deep and unstable boundary layers allow high stack emissions (emitted above the boundary layer during winter) to reach the ground in close proximity to point sources. Diurnal profiles of PM_{10} and $PM_{2.5}$ display maxima during morning (06:00–09:00 LT) and evening (17:00–22:00 LT) at nearly every site – especially during winter – and underscore the importance of domestic burning as a major source of primary particles. Multi-year averages indicate that evening maxima at some township sites average in excess of $400\,\mu g\,m^{-3}$. These results from the urban/industrial Gauteng area quantitatively confirm previous studies suggesting that the lowest-income populations of South Africa experience the poorest air quality, and demonstrate that domestic burning results in frequent exposure to high concentrations of particulate pollution in the region comprising the cities of Johannesburg and Tshwane.

While remotely-sensed data are frequently used as a proxy for ground air quality, we report poor correlations between PM concentrations and satellite parameters and suggest that this practice is not appropriate in metropolitan South Africa. Disagreement between satellite and ground data may be attributed to a number of factors: (1) vertical inhomogeneity and stratified pollution layers aloft during much of the year, (2) extremely shallow winter boundary layers, (3) discrepancy between satellite passover times and elevated diurnal PM concentrations, and (4) poor spatial resolution of satellites compared with highly localized PM sources. While remotely-sensed data provide a good picture of regional, seasonal properties of column aerosol, a complete understanding of South Africa's air quality at the ground will necessitate more extensive monitoring

Title Page

Abstract	Introduction
Conclusions	References
Tables	Figures

Back | Close

Full Screen / Esc

Printer-friendly Version

Interactive Discussion

at the ground and intensive, multi-platform campaigns to understand the relationship between ground and satellite data.

1   Introduction

The impacts of aerosols on human health, visibility, and climate are well-documented. There are a number of natural sources of dust, sea salt, sulfate, and organic aerosol, but those most detrimental to human health are particles derived from anthropogenic fuel burning activities. Combustion aerosol can be directly emitted as soot or formed in the atmosphere through photochemical reactions that produce low-volatility, secondary sulfate, nitrate, and organic species that either nucleate to form new aerosol or condense onto existing particles. Exposure to particulate pollution is typically worst in urban areas, where anthropogenic emissions are collocated with high population density. The lowest-income fraction of the population tends to experience the worst air quality because the least expensive property (or land available for informal settlements) is often close in proximity to major air pollutant sources like highways, power generation facilities, or industry. In developing countries, low-income households are significantly more likely to utilize non-electricity energy sources such as coal, wood, and paraffin (FRIDGE, 2004; Pauw et al., 2008). Suboptimal burning conditions in domestic settings often result in large emissions of particulates and particulate precursors, leading to high concentrations of PM (FRIDGE, 2004; von Schirnding et al., 2002; Yeh, 2004). In South Africa, the highest concentrations of PM_{10} and $PM_{2.5}$ are measured in townships and informal settlements during winter, when domestic burning is most prevalent for heating and cooking, and when emissions are confined in a shallow boundary layer (FRIDGE, 2004; von Schirnding et al., 2002; Yeh, 2004; Wichmann and Voyi, 2005). A number of reports and peer-reviewed articles have sought to characterize air quality in low-income areas of South Africa (e.g., Engelbrecht et al., 2000, 2001, 2002; FRIDGE, 2004; Pauw et al., 2008), but these studies have typically been limited in ge-

ographic scope and have not characterized the major metropolitan centers where high densities of South Africans reside.

There is a wealth of remotely-sensed air quality information available from satellite platforms, and a number of studies have used aerosol optical depth (AOD or τ) as a proxy for air quality (Zhuang et al., 2014; Luo et al., 2014; Zhang et al., 2014; Qi et al., 2013; Massie et al., 2006; Kumar et al., 2013; Alam et al., 2011; Kaskaoutis et al., 2007; Carmona and Alpert, 2009; Guo et al., 2011; Marey et al., 2011; Sorooshian et al., 2011; Tesfaye et al., 2011; Sreekanth and Kulkarni, 2013; Singh et al., 2004; Crosbie et al., 2014). AOD typically displays strong seasonality, with higher AOD observed during periods of peak photochemical production of secondary aerosol – except in areas where either dust generation or biomass burning enhances AOD during other seasons. AOD frequently correlates with ground-based observations of visibility and particulate concentrations, suggesting that it may be an appropriate surrogate for particulate matter at the ground in a number of regions. However, vertical variability in particulate concentrations makes the use of AOD as a proxy for surface air quality tenuous. For example, concentrated plumes of particles transported aloft may enhance AOD significantly but not impact air quality at the ground (e.g., Campbell et al., 2003). Conversely, high concentrations of pollutants in a shallow boundary layer with particle-free air aloft will result in low AOD despite extremely poor air quality at the ground (e.g., Crosbie et al., 2014). While remotely-sensed AOD may provide an appropriate measure of air quality in some areas, its general applicability must be evaluated and caution must be exercised when attempting to use column aerosol data as a surrogate for ground particulate concentrations.

Particulates measured at the ground in South Africa are predominately dust, industrial secondary sulfate, and secondary organics (Piketh et al., 2002; Tiitta et al., 2014), but significant attention has been paid to the impact of biomass burning on particulates in the country. Regional biomass burning in Southern Africa occurs from June to October (Cooke and Wilson, 1996), and impacts AOD in South Africa during August and September (Formenti et al., 2002, 2003; Campbell et al., 2003; Eck et al.,

Title Page

Abstract | Introduction

Conclusions | References

Tables | Figures

◀ | ▶|

◀ | ▶

Back | Close

Full Screen / Esc

Printer-friendly Version

Interactive Discussion

2003; Ross et al., 2003; Winkler et al., 2008; Magi et al., 2009; Queface et al., 2011; Tesfaye et al., 2011; Kumar et al., 2013). The biomass burning emissions that most significantly impact South Africa originate in neighboring countries – particularly Zimbabwe and Mozambique (Magi et al., 2009). Because these emissions are transported in stratified layers aloft (Campbell et al., 2003; Chand et al., 2009), they may impact column aerosol properties such as AOD but not particulate concentrations at the ground. While transported biomass burning has been demonstrated to impact AOD seasonally, domestic burning – especially for heating and cooking during winter – is the source associated with the highest particulate concentrations in South Africa (Engelbrecht et al., 2000, 2001, 2002). Despite work to characterize emission factors and ambient air quality impacts of domestic burning, studies have been limited in scale to the household or township level and have never considered the dynamics and impact of domestic burning emissions across an entire major population center.

Here, we focus on air quality characteristic of urban centers in South Africa. First we present remotely-sensed and modeled column aerosol data related to total light extinction (AOD), particle size (Ängström Exponent, α), total light absorption (ultraviolet aerosol index, UVAI), and AOD contribution from individual chemical components (Goddard Ozone Chemistry Aerosol Radiation and Transport, GOCART). Satellite data are focused on the five metropolitan and industrial areas of South Africa with highest population density (Cape Town, Bloemfontein, Gauteng Province, Industrial Highveld Air Quality Priority Area or HVAPA, and Durban). We then investigate ground-based measurements of particulate matter (PM_{10} and $PM_{2.5}$) within the satellite study area that comprises the Johannesburg and Tshwane metropolitan areas (Gauteng Province) in order to understand seasonal, diurnal and regional trends in particulate concentrations across the primary environment types common to all major South African population centers: townships, urban/suburban residential areas, and industrial areas. We finally explore connections between remotely-sensed and ground data in order to determine whether satellite-derived air quality parameters are appropriate surrogates for air quality at the ground in the South African context.

2 Data and methods

This study utilizes a combination of remotely-sensed and ground-based observations of atmospheric particulates across South Africa. Rather than define study areas based on large geographical regions that require significant data averaging (e.g., Tesfaye et al., 2011), we focused our study of remotely-sensed data on five smaller study areas that comprise the five major metropolitan centers of population density in South Africa (Cape Town, Bloemfontein, Gauteng Province, Industiral Highveld Air Quality Priority Area or HVAPA, and Durban; Fig. 1). We then utilized data from four networks of ground-based air quality monitoring from the South African Air Quality Information System (SAAQIS) for one of these study areas (Gauteng; see Table 1) in order to determine local and diurnal trends in PM_{10} and $PM_{2.5}$ and to determine the extent to which remotely-sensed measurements of atmospheric particulates are able to capture trends in PM concentrations that are observed at the ground in densely-populated urban areas. When seasonal characteristics are described, Southern Hemisphere summer is defined as December–February (DJF), fall is March–May (MAM), winter is June–August (JJA), and spring is September–November (SON).

2.1 Remotely-sensed aerosol data

Remotely-sensed aerosol data from Moderate Resolution Imaging Spectroradiometer (MODIS) Version 5.1 (Remer et al., 2005), Multi-angle Imaging Spectroradiometer (MISR) Version 31 (Diner et al., 2001b, a), and Total Ozone Mapping Spectrometer (TOMS) Version 8 (Herman et al., 1997) were obtained from NASA's Giovanni Data and Information Services Center (http://disc.sci.gsfc.nasa.gov/giovanni). Data from MODIS included $1° \times 1°$ gridded cloud fraction, aerosol optical depth (AOD or τ) at 550 nm from both the Aqua and Terra platforms (AOD_{550}), and Ängström Exponent (α) with Aqua representing spectral dependence of AOD between $\lambda = 550$ and 865 nm and Terra between $\lambda = 470$ and 660 nm. MODIS data were available between 1 March 2000 and 31 December 2009 (Terra) and 4 July 2002 and 31 December 2009 (Aqua). MODIS

data included daily 1° × 1° gridded Deep Blue AOD at 550 nm (Hsu et al., 2004), which is a retrieval algorithm capable of distinguishing particles over bright land surfaces and returning AODs within 20–30 % of ground-based sun photometers (Hsu et al., 2006). Data from MISR included 0.5° × 0.5° gridded AOD at 555 nm (AOD_{555}) and were obtained for the period 25 February 2000 to 31 December 2009. Ultraviolet Aerosol Index at 1° × 1.25° was obtained from TOMS for the period 24 February 2000 to 14 December 2005, utilizing a minimum UVAI threshold of 0.5 to account for retrieval uncertainties. For all remotely-sensed data, a filter was applied to use only data corresponding to cloud fraction < 70%.

2.2 Goddard Ozone Chemistry Aerosol Radiation and Transport (GOCART) model

Data from the Goddard Ozone Chemistry Aerosol Radiation and Transport model (GO-CART; Chin et al., 2002) were used to determine modeled contribution to total AOD_{550} by individual aerosol components: black carbon, organic carbon, dust, sulfate, and sea salt. Resolution was 2° × 2.5° and data were available between 24 February 2000 and 31 December 2007.

2.3 Satellite fire data

Data from the MODIS Fire Information for Resource Management System (FIRMS) provided a climatology of burn frequency and intensity over southern Africa (0 to 35° S and 5 to 55° E) between 1 January 2000 and 31 December 2009. FIRMS data are available for each MODIS overpass and lists the location of identified fires along with fire characteristics which includes fire radiative power (FRP), which captures the intensity of burning within each fire pixel. To capture the frequency and geographical range of burning together with intensity, we report time average FRP integrated at a resolution of 0.5° × 0.5°.

2.4 Airmass back-trajectory data

NOAA's Hybrid Single-Particle Lagrangian Integrated Trajectory (HYSPLIT) model (Draxler and Rolph, 2003) was run using NCAR/NCEP reanalysis data with the isentropic vertical velocity method in order to determine air mass origin for the Gauteng satellite grid box. Trajectories were obtained from 1 January 2000 through 31 December 2009 ending at the center of the box (26° S, 28° E) at 500 m above the surface. Seasonal trajectory frequency maps were constructed for fall (March–May), winter (June–August), spring (September–November), and summer (December–February) in order to illustrate the most frequent source areas for air arriving in the Gauteng region and aid in interpreting combined satellite and ground results for the region.

2.5 Ground data

Hourly ground-based air quality data were obtained from four different networks reporting to the South African Air Quality Information System (SAAQIS), all located within the Gauteng satellite grid box. Table 1 categorizes individual ground monitoring sites according to both the monitoring network and site type to which they belong, and gives date ranges and data available. Site classifications were made on the basis of site descriptions on the SAAQIS website (available at: http://www.saaqis.org.za/NAAQM.aspx), site visits, and personal correspondence with the NGO NOVA Institute, which works extensively in townships and informal settlements. Data were used as per approval from each monitoring network, and were subject to data quality controls. Negative values were discarded, as well as "repeat" values with the same value given for many hours at a time. Where > 30% of data points were missing over a given time-averaging period, data were discarded.

2.6 Meteorology data

Hourly ground-based meteorology observations were obtained through the South African Weather Service (SAWS) for 5 sites corresponding to each of the 5 major metropolitan study areas considered in the study. Data include pressure, precipitation, temperature, relative humidity, wind direction, and wind speed from Cape Town (33.98° S, 18.60° E; 1 April 2001 through 31 December 2009), Bloemfontein (29.12° S, 26.19° E; 25 December 2000 through 31 December 2009), Johannesburg (26.15° S, 28.00° E; 25 December 2000 through 31 December 2009), Ermelo (26.50° S, 29.98° E; 25 December 2000 through 31 December 2009) and Durban (29.97° S, 30.95° E; 25 December 2000 through 31 December 2009).

3 Results and discussion

3.1 Study areas: land use and emissions

Locations and sizes of study areas are displayed in Fig. 1. Zoom-in outsets show land use percentage and major emissions sources for each region. In every region are significant area sources corresponding to biomass burning (veld fires that occur in early- to mid-winter) and informal settlements (primarily domestic burning throughout the winter). Mine tailings and waste dumps from gold mining are prevalent in Gauteng, with emissions dependent on wind speed. Petroleum refineries are major point sources in Gauteng, HVAPA and Durban, with some presence in Cape Town. Coal-fired power plants are prevalent through Gauteng and HVAPA, and are collocated with open mining along coal deposits in the region. Overall, Gauteng and HVAPA have by far the highest density of anthropogenic emissions from all sources, including significant on-road emissions.

3.2 Satellite and model results

A number of satellite and model products are available through NASA's Giovanni Data and Information Services Center (http://disc.sci.gsfc.nasa.gov/giovanni). We focus here on products related to atmospheric particulates, presenting decade-averages (01 January 2000 to 31 December 2009 or some multi-year subset, depending on data availability) of Aerosol Optical Depth (AOD or τ), Ängström Exponent (α), Ultraviolet Aerosol Index (UVAI), and chemical component contributions to AOD from The Goddard Chemistry Aerosol Radiation and Transport (GOCART) model. Each of these parameters describes a unique aspect of the aerosol column, and results will be presented as follows: (i) a brief description of the parameter, (ii) general regional and seasonal trends, and (iii) discussion of those trends, incorporating other data platforms to support conclusions where appropriate. Main conclusions are synthesized in Sect. 4, and satellite data are summarized in Table 2.

3.2.1 Aerosol Optical Depth (AOD)

AOD_{550} from the MODIS (Aqua and Terra) and AOD_{555} MISR satellite platforms, and total AOD predicted by GOCART are presented in Fig. 3. AOD is a measure of the reduction of intensity of light due to scattering and absorption of particles along path length, and is defined for a specific height (z) and wavelength (λ) according to the Beer–Lambert law:

$$\frac{F(z,\lambda)}{F_{TOA}(\lambda)} = \exp(-\tau(z,\lambda)), \tag{1}$$

where transmittance, or $F(z,\lambda)/F_{TOA}(\lambda)$, is the ratio of radiation intensity at height z to intensity at the top of atmosphere (TOA), for a given wavelength λ. Here, z is the entire atmospheric path length between the ground and TOA, and λ is 550 nm for both MODIS platforms (Aqua and Terra) and 555 nm for MISR. Typical values of $AOD_{550,555}$

South African aerosol

S. P. Hersey et al.

Title Page

Abstract	Introduction
Conclusions	References
Tables	Figures

|◄ | ►|

◄ | ►

Back | Close

Full Screen / Esc

Printer-friendly Version

Interactive Discussion

range from 0.05 in remote, clean environments to 1.0 in areas of extreme particle concentrations.

AOD is a function of particle extinction efficiency (Q_{ext}) and particle number distribution. First considering extinction efficiency, Q_{ext} is the sum of scattering and absorption efficiencies ($Q_{ext} = Q_{scat} + Q_{abs}$). Q_{scat} increases proportional to particle diameter to the 4th power (D_p^4) as particle size increases relative to λ, meaning that extinction efficiency and thereby AOD increase rapidly with particle diameter. Because Q_{abs} increases only proportionally to D_p, even small absorbing particles ($< 0.1\,\mu m$) can exhibit high absorption efficiency and thereby impact τ significantly. In addition to extinction efficiency, particle number distribution (particle concentration at specific sizes) has a second-order relationship with AOD, such that aerosol size distributions dominated by larger particles ($D_p > \lambda$) such as dust tend to have significantly higher AOD than those dominated by smaller particles (smaller than λ). Considering these influences on AOD, one can conclude that low values of AOD (< 0.1) correspond to relatively clean conditions with low particle concentrations, few large particles and aerosol number distributions comprised primarily of small, non-absorbing particles. One may also conclude that large values of AOD correspond to high concentrations of large particles such as dust, high concentrations of absorbing aerosol at any size, or some combination of the two.

Discrepancies in AOD between satellite platforms are generally within uncertainty, and arise due to differences in factors such as processing methods (Abdou et al., 2005), calibration and retrieval algorithms (Kahn et al., 2007), and even measurement time (Terra and MISR pass over South Africa between 09:00 and 11:00 LT, while Aqua passes over between 13:00 and 15:00 LT). In this study, Terra and Aqua AOD_{550} are well-correlated with AOD_{555} from MISR, with Pearson's R correlation coefficients (r) > 0.7, except in Cape Town and Bloemfontein ($r = 0.36$ and 0.59, respectively). Because trends in AOD_{550} and AOD_{555} are similar and highly correlated in most sites, we will refer to "AOD" without specifying wavelength, except when highlighting wavelength-dependent trends in the data. Total AOD_{550} modeled by GOCART correlates well with all satellite platforms in all sites ($r > 0.7$). In Cape Town and Durban, MISR AOD_{555} ap-

Title Page

Abstract | Introduction

Conclusions | References

Tables | Figures

|◄ | ►|

◄ | ►

Back | Close

Full Screen / Esc

Printer-friendly Version

Interactive Discussion

pears significantly higher than either MODIS platform or GOCART. The surface at both of these sites displays a great deal of heterogeneity, with satellite grid boxes extending over both bright land and dark ocean surfaces. While estimated biases between MISR and MODIS are expected to be low over uniformly dark surfaces (Kahn et al., 2007), assumptions about surface reflectivity tend to introduce significant discrepancies with increased surface heterogeneity (Chu et al., 2002). MISR is less sensitive to surface characteristics, and so in regions with significant heterogeneity such as Cape Town or Durban, one may expect AOD_{555} from MISR to be more accurate.

Considering Fig. 3, AOD_{550} is consistently lower in Cape Town than other major metropolitan areas of South Africa, owing to frequent air mass origin over clean marine areas and minor influence by large or absorbing aerosols. At continentally-influenced sites (Bloemfontein, Gauteng, HVAPA, and Durban), there is a maximum in AOD_{550} and AOD_{555} between 0.12 and 0.20 from late winter to early spring. AOD is moderate through summer, averaging 0.08–0.17, and reach a minimum during late fall and early winter (MJJ), with AOD ranging from 0.05–0.10. AOD is particularly high in magnitude and variability in Durban between August and October, with MISR AOD_{555} showing monthly averages approaching 0.3. The seasonal trends evident in Fig. 3 can be explained by considering annual variability in: (1) biomass burning and (2) dust generation. The impact of these parameters on AOD is explored below.

The first and most distinct annual feature across South African metropolitan areas is the August–October maximum in AOD. This maximum coincides with the burning season in Southern Africa, which has been identified as major regional source of transported aerosol in South Africa (Piketh et al., 1999, 2002; Formenti et al., 2002, 2003; Eck et al., 2003; Ross et al., 2003; Campbell et al., 2003; Winkler et al., 2008; Magi et al., 2009; Queface et al., 2011). Figure 2 presents average monthly fire counts per km^2 from 2000–2010 in Sub-Saharan Africa, and indicates that the most significant burning in Southern Africa occurs between May and September and is located in the tropics (between 0 and 20° S). These fires are massive sources of biomass burning emissions that are often transported in stratified layers aloft (Campbell et al., 2003)

and significantly impact column aerosol optical properties like AOD in South Africa (Formenti et al., 2002; Magi et al., 2009). Winkler et al. (2008) demonstrated that these transported biomass burning emissions represent the dominant source of irradiation losses during late winter and early spring in South Africa, and Queface et al. (2011) in-

5 dicated that transported fire emissions are the bulk of column aerosol loading between August and October. Strong north-to-south gradients in AOD are observed during the burning season, with significantly higher AOD near sources, where aerosols are small, but highly absorbing and concentrated (Eck et al., 2003; Campbell et al., 2003). Lower AOD is typically observed at downwind receptor sites after plumes have evolved to

10 comprise less absorbing and predominantly Aitken and accumulation mode particles with sufficient condensed water-soluble secondary aerosol species for the particles to serve as CCN (Ross et al., 2003; Eck et al., 2003). It follows, therefore, that AOD in South Africa is enhanced most significantly by close-proximity fires within South African borders and in neighboring Mozambique and Zimbabwe. These close-proximity fires

15 reach their peak frequency in August, September, and October and coincide with the maxima in AOD observed across all continentally-influenced sites in this study. Because AOD is highest in closest proximity to fires, the influence of biomass burning on AOD is expected to be strongest nearer sources in eastern South Africa. Proximity explains the high magnitude and variability of AOD in Durban between August and

20 October, where very close proximity sugar cane field burning typically occurs, releasing high and variable concentrations of absorbing biomass burning particles (LeCanut et al., 1996). In all sites AOD reaches a minimum of 0.05–0.10 in late fall and early winter (MJJ), despite evidence of wintertime enhancements in emissions and concentrations of PM_{10} from domestic burning for heating and cooking (Engelbrecht et al.,

25 2000, 2001, 2002; Winkler, 2007; Bigala, 2009; Mdluli, 2007; Pauw et al., 2008; Venter et al., 2012). This suggests that these domestic emissions, which occur close to the ground in a shallow boundary layer, have little influence on column aerosol properties.

Next, elevated AOD in August and September coincides with a period of enhanced generation of windblown dust across South Africa. Ground-based meteorology data

Title Page

Abstract | Introduction

Conclusions | References

Tables | Figures

◀ | ▶

◀ | ▶

Back | Close

Full Screen / Esc

Printer-friendly Version

Interactive Discussion

from South African Weather Service (SAWS) monitoring sites in each region are presented in Fig. 5, and indicate that in all regions but Cape Town, wind speeds increase in July and August before an enhancement in precipitation in September and October. High winds combined with dry conditions result in generation of wind-blown dust particles, which are both large and strongly absorbing and thereby have strong bearing on AOD. Enhanced AOD coincides with dust generation in August and September, and we therefore suggest that dust may be an additional, previously underestimated factor influencing AOD across South Africa.

Column water vapor (CWV) derived from the Modern Era-Retrospective Analysis for Research and Applications (MERRA; Rienecker et al., 2011) was analyzed for each site in order to determine whether enhanced water vapor might be a factor contributing to elevated AOD through a mechanism of hygroscopic growth of particles. However, no significant correlation was found between AOD and CWV in any site, supporting findings in Kumar et al. (2013), which found no relationship between the two parameters at a site in rural, northeastern South Africa. Further, AOD in Gauteng and HVAPA is not significantly higher than other sites despite these regions having the highest concentration of anthropogenic sources. This suggests that anthropogenic aerosol in these regions comprises small, non-absorbing particles that have little impact on AOD.

Overall, AOD_{550} and AOD_{555} values reported here are consistent with those reported by Tesfaye et al. (2011) based on broad, regionally-averaged 10-year MISR AOD_{555} trends for northern, central, and southern regions of South Africa. The observation of enhanced AOD associated with transported biomass burning aerosol also agrees with similar trends for central and northern South Africa in that work. But overall, AOD_{550} and AOD_{555} are lower than many previously-published values over Southern Africa. Queface et al. 2011 reported long-term, monthly-averaged AOD_{550} ranging from 0.10 to over 0.6 at a site near dense biomass burning sources in Zambia, and monthly averages between 0.17 and 0.30 at a site in northeastern South Africa near the Mozambique border. A strong N–S gradient in AOD_{550} is typically observed during biomass burning season in Southern Africa (Eck et al., 2003), with sites to the north experienc-

ing significantly higher AOD than sites in the south due to closer proximity to sources. This suggests that while transported biomass burning aerosol has a clear impact on AOD across the major metropolitan areas of South Africa (except Cape Town), this impact is nonetheless much less pronounced than for sites farther to the north and closer to denser burning sources.

As AOD is frequently used as a proxy for megacity anthropogenic particulate pollution, it is important to view results from South Africa within the context of worldwide megacities. Considering the major metropolitan and industrial areas of Gauteng and HVAPA, seasonally-averaged AOD_{550} ranged from a minimum of 0.12 in winter to a maximum of 0.17 in spring – values that are a factor of 3–6 lower than those typical of megacities and major industrial areas worldwide. Annual averages of AOD_{550} in industrialized and urban areas of Hong Kong and China such as Nanjing, the North China Plain, and Yangtze River, for example, are on the order of 0.6–0.8 (Zhuang et al., 2014; Luo et al., 2014; Zhang et al., 2014). AOD_{550} in Mexico City ranges from a seasonally-averaged minimum of 0.2 to a maximum of 0.6 (Massie et al., 2006), and in the Dheli region of India AOD_{550} ranges from a seasonal minimum of 0.4 to a maximum during monsoon season of 1.4. So while the Gauteng area and HVAPA areas have been identified as a megacity from the standpoint of NO_x emissions (Beirle et al., 2004; Lourens, 2012), it does not appear to be a hotspot for regional particulates.

3.2.2 Ängström Exponent (α)

Monthly-averaged Ängström Exponent (α) from the MODIS Aqua and Terra platforms is presented in Fig. 6. α captures the spectral dependence of aerosol extinction based on measurements of AOD at two different wavelengths:

$$\alpha = -\frac{\mathrm{dlog}\tau}{\mathrm{dlog}\lambda} = -\frac{\log(\tau_1/\tau_2)}{\log(\lambda_1/\lambda_2)}, \tag{2}$$

where $\tau_{1,2}$ are AODs at wavelengths $\lambda_{1,2}$. For small particles in the Rayleigh scattering regime ($D_p < 0.1\,\mu m$), AOD scales with wavelength as ($1/\lambda^3$ to $1/\lambda^4$), and $\alpha > 2$ where

fine particles dominate. Large particles, on the other hand, are more spectrally neutral and the lack of wavelength dependence of scattering and absorption results in $0 < \alpha < 1$ where coarse particles dominate. α is reported for both MODIS platforms, with Aqua representing spectral dependence of AOD between $\lambda = 550$ and 865 nm and

5   Terra between $\lambda = 470$ and 660 nm. α is quantized in such a way that it cannot be used as a quantitative metric for aerosol size integrated through the column (Remer et al., 2005; Levy et al., 2010). Instead, we interpret α results as being qualitatively indicative of the aerosol type present in the column – either fine (values close to 2) or coarse (values between 0 and 1). Due to the qualitative nature of the variable, combined with

10   the fact that $\alpha_{550/865}$ and $\alpha_{470/660}$ are highly correlated ($r > 0.8$) in all sites, we will refer to α without specifying wavelength except where specifically relevant.

    Considering Fig. 6, α shows similar trends to AOD (Fig. 3). Generally there is a maximum in α of 1.0–1.8 during spring and through summer, gradually decreasing through fall to reach a minimum of 0.6–1.0 in winter. This suggests that fine particles are most

15   abundant in the column in spring when biomass burning impacts South Africa, agreeing with previous results suggesting that aerosol plumes transported to South Africa from dense burning areas to the north tend to be characterized by mainly Aitken mode (0.01–0.1 µm) aerosol (Eck et al., 2003; Formenti et al., 2003). α remains high through the hot, photochemically intense summer months, when significant fine, secondary

20   sulfate, nitrate, and organic aerosol is produced from abundant industrial emissions of SO_2, NO_x, and VOCs, respectively (Piketh et al., 1999; Hirsikko et al., 2012), and when as many as 86 % of days in industrial areas display new particle formation (Hirsikko et al., 2012). This is in contrast to the dry winter months, when α is low and it appears as though particles above the major metropolitan areas of South Africa tend

25   to be larger – perhaps with a greater contribution from dust or large soot particles. α is relatively constant throughout the year in Cape Town, indicative of a consistent aerosol size distribution resulting from clean, marine airmass origin and fairly constant local generation of marine aerosol. At the other coastal cite (Durban), α is similarly high throughout the year, but displays the strong seasonal biomass burning signal in spring

owing to its location to the east of South Africa, nearer major biomass burning sources of small particles in Zimbabwe and Mozambique and in close proximity to springtime sugar cane burning.

In addition to a clear impact on α by transported biomass burning emissions, maxima and minima in α are highly correlated with CWV in all regions except Cape Town (Fig. 4; $0.64 < r < 0.98$). This result agrees with Kumar et al. (2013), who found that CWV correlated well with α, but not AOD. The relationship between CWV and α is unlikely to be causal, but rather coincidental since wet summer months tend to have less dust generation (fewer large particles and higher α) and enhanced secondary photochemical aerosol production (more small particles and higher α). Overall, α for inland sites (Bloemfontein, Gauteng, HVAPA) is significantly lower on average than for coastal sites (Cape Town and Durban), with $\alpha < 1$ for much of the year. This suggests that coarse particles such as dust form an important contribution to column aerosol loading, and appear to dominate the aerosol column during winter for inland sites.

Values of α reported here are lower than previously reported in Southern Africa, primarily because major studies of aerosol optical properties in the region have focused on intensive periods of biomass burning. Eck et al. (2003) found high α near biomass burning sources in Zambia (1.8–1.9) during biomass burning season from August–October, while Robles-Gonzalez et al. (2008) measured α as high as 2.1 in burning regions. Kumar et al. (2013) found strong seasonal variability at a site in northeastern South Africa, with high α (up to 2.9) during burning season, but much lower α (0.5) during the rest of the year. Ranges of α similar to those reported here have been observed in urban and industrial sites in China (ranging from 0.5–1.6 in Qi et al., 2013, with an annual average of 1.25 in Zhuang et al., 2014).

3.2.3 Ultraviolet Aerosol Index (UVAI)

Month averages of Ultraviolet Aerosol Index (UVAI) from the Total Ozone Mapping Spectrometer (TOMS) are presented for each region in Fig. 7. UVAI is a qualitative metric based on the difference between the ratio of absorbing and non-absorbing spectral

radiance ratios provided by satellite observations and model calculations. High values of UVAI are associated with high concentrations of strongly absorbing aerosols – namely UV-absorbing soot, smoke, and mineral dust (Hsu et al., 1996), as well as ash and brown carbon. UVAI reaches a maximum of 1.0–1.2 in spring and remains high through summer before decreasing to a minimum of 0.7 during winter. This trend underscores the influence of strongly-absorbing biomass burning and dust aerosol, which are most prevalent through spring. Trends in UVAI generally follow those of AOD (Fig. 3) and exhibit good correlation with MISR AOD ($r \sim 0.6$), except for the Cape Town region where marine aerosol appears to influence column aerosol dynamics. The only statistically significant difference between sites is observed in Durban during August and September, when UVAI is elevated relative to other sites owing to significant emissions of strongly-absorbing biomass burning emissions from local sugar cane burning (LeCanut et al., 1996).

3.2.4 Goddard Ozone Chemistry Aerosol Radiation and Transport (GOCART) model

GOCART model results estimate the contribution of dust, black carbon, organic carbon, sulfate, and sea salt to total column AOD, based on global emissions inventories (Chin et al., 2002). Total estimated GOCART AOD is presented in Fig. 3, and the fraction of AOD attributed to each modeled constituent is displayed in Fig. 8. The monthly-averaged fractional contribution of each aerosol component is very consistent across sites, displaying high r for individual components (i.e. dust in Joburg compared with dust in Durban for a particular month); typically ~ 0.9. Only Cape Town exhibits a unique trend, owing largely to the significantly larger modeled contribution of dust throughout the year. Modeled dust enhancement in Cape Town is especially pronounced from May through July, when emissions inventories include a large contribution from windblown dust from the nearby Namib Desert. Such an enhancement in the contribution of dust would presumably result in an enhancement in UVAI during May–July and a general trend of elevated UVAI in Cape Town, which is not observed in

the data. Further, GOCART results do not capture the enhancement in dust aerosol expected in late winter to early spring (JAS) based on AOD, UVAI, and enhanced ground wind speed in dry conditions. We therefore suggest that GOCART emissions inventories either significantly overestimate dust in Cape Town or underestimate dust emissions for the rest of South Africa. Given the consistent UVAI across sites in Fig. 7, the strong potential for dust generation in early spring when winds increase but before precipitation arrives, and previous work indicating that > 70 % of coarse and > 40 % of fine particle mass is contributed by dust at sites in the Eastern Cape and Highveld (Piketh et al., 1999, 2002), we suggest that GOCART significantly underestimates dust as an aerosol source over the majority of metropolitan areas in South Africa.

3.3 Ground-based sampling results

Ground-based air quality data were obtained through monitoring networks within the Gauteng satellite grid box comprising the cities of Johannesburg and Tshwane (Pretoria). Table 1 summarizes data type and date ranges available for sites utilized in this study. Sites were classified as one of four types: township or informal settlement sites characterized by some domestic burning emissions (Township/Domestic Burning), developed residential areas in either urban or suburban settings with no domestic burning emissions (Urban/Suburban Residential), areas rich with industrial or power generation activities (Industrial), or sites aimed at capturing on-road sources (Traffic). An emissions summary for the Gauteng area (Fig. 1) indicates that the most significant area sources are from biomass burning (veld fires that occur in early- to mid-winter), informal settlements (primarily domestic burning throughout the winter), and mine tailings and waste dumps (emissions dependent on wind speed). The most significant point sources in Gauteng are three coal-fired power plants and two petrochemical refineries in the south, and five steel manufacturing facilities and three cement manufacturing facilities to the south and central part of the region.

Seasonally-averaged HYSPLIT back-trajectory frequencies (Fig. 9) indicate typical air mass origin for Gauteng. Summer and fall are characterized by air arriving from the

east and southeast, while winter is directionally distributed and spring typically sees air transported from the north and east (Zimbabwe and Mozambique), with some contribution from the southwest and southeast. Local meteorology for Gauteng (Fig. 5) was described above and is characterized by cool and very dry winters, with temperature and precipitation increasing through the spring to maxima in the summer. Wind speed increases before precipitation in the spring, resulting in local dust generation from July through September.

Monthly averages of PM_{10} and $PM_{2.5}$, both in absolute magnitude and normalized by each site's maximum monthly average, are presented in Fig. 10. PM concentrations reach a maximum in winter (June, July, or August) for all sites except industrial areas. This maximum in PM concentrations corresponds to the coldest months, when the most significant domestic burning activity is expected and boundary layers are extremely shallow (often 50 m or less). The summer maximum in industrial areas may result from photochemistry of industrial precursors and generation of secondary particulates, or may be due to atmospheric dynamics. During winter, industrial stack emissions tend to be released far above the very shallow boundary layer and into stable atmospheres. During summer, on the other hand, deeper boundary layers extend above stacks and industrial emissions therefore stay within a less stable boundary layer, resulting in mixing of emissions down to the ground. The average monthly ratio of $PM_{2.5}$ to PM_{10} was calculated for sites with both parameters, and there is no statistically significant monthly trend, suggesting that fine particles comprise a relatively consistent fraction of total particulate concentration throughout the year, despite large changes in overall particulate concentration.

Diurnal averages of PM_{10} and $PM_{2.5}$ for each season are presented in Fig. 11. PM_{10} and $PM_{2.5}$ concentrations have been normalized by the maximum hourly average for each site for the entire year (typically 19:00–21:00 LT during winter), with the average concentration (in absolute magnitude) for each type of site displayed in the third row of diurnal plots. As was evident in monthly PM data, the highest concentrations occur in township areas where domestic burning is expected, followed by significantly lower PM

South African aerosol

S. P. Hersey et al.

Title Page

Abstract	Introduction
Conclusions	References
Tables	Figures

Back | Close

Full Screen / Esc

Printer-friendly Version

Interactive Discussion

concentrations in urban and suburban residential areas and the lowest concentrations on average in industrial areas. The clearest feature in the diurnal data is the significant enhancement in particulate concentrations in the morning (06:00–09:00 LT) and evening (17:00–22:00 LT) during all seasons. This trend is especially dramatic during winter, with typical evening PM_{10} and $PM_{2.5}$ concentration maxima in township areas of 203 and 105 $\mu g\,m^{-3}$, respectively, with evening PM_{10} maxima averaging in excess of 400 $\mu g\,m^{-3}$ at some sites. That these diurnal patterns of enhanced PM concentration in morning and evening discernible in all seasons is evidence that domestic burning impacts air quality in South Africa throughout the year, but the significant enhancement in PM during winter underscores the fact that increased burning during cold months within shallow boundary layers consistently leads to dangerous concentrations of particulates – particularly in the lowest-income residential areas. It should be mentioned that the observed diurnal patterns may also reflect some contribution from on-road emissions – either primary combustion or vehicle-associated dust particles. However, the high density of domestic burning and relatively low density of vehicles in townships compared with other areas suggests that these on-road sources should be minor compared with primary burning emissions. The diurnal ratio of $PM_{2.5}$ to PM_{10} is displayed in Fig. 11, and reaches a minimum at all township sites between 12:00 and 15:00 LT, indicating that morning and evening domestic burning activity tends to be a source of small particles.

Diurnal and monthly maxima, minima, and mean values for both PM_{10} and $PM_{2.5}$ are presented in Table 3. On average, PM concentrations in townships are 51 % higher than urban/suburban residential sites and 78 % higher than industrial sites, underscoring the importance of domestic emissions as associated with the highest concentrations of particles in the region. The difference between townships and other areas is more distinct in winter, when PM concentrations in townships are 63 and 135 % higher than in urban/suburban residential and industrial sites, respectively. The average wintertime evening maximum in PM_{10} of 203 $\mu g\,m^{-3}$, approaching 400 $\mu g\,m^{-3}$ at many township sites, is 50–250 % higher than 24 h PM_{10} standards set by the United States

South African aerosol

S. P. Hersey et al.

Title Page

Abstract | Introduction

Conclusions | References

Tables | Figures

|◄ | ►|

◄ | ►

Back | Close

Full Screen / Esc

Printer-friendly Version

Interactive Discussion

Environmental Protection Agency, South African Department of Environmental of Affairs, and the World Health Organization (150, 180, and 50 µg m^{-3}, respectively). There is significant variability in PM concentrations between sites just a few kilometers apart, indicating that the domestic burning that generates the highest concentrations of particulates is highly localized and most dramatically impacts air quality in a small area in the immediate vicinity of emissions. This result indicates that domestic burning PM source strength in low-income areas is highly variable, depending on factors such as the availability of electricity, the method of burning coal or wood, and thermal efficiency of homes.

Data from two township sites (Alexandra and Bodibeng) have diurnal trends that do not conform to the typical morning and evening PM enhancements typical of low-income areas, and represent intriguing case studies in the impact of township evolution and informal commercial activity within the township context. Alexandra was established in 1912 and in recent years has become fully electrified with paved roads and significant formal and informal commercial activity throughout the day. As the township has developed, residents have almost ubiquitously adopted electricity as the only energy source for both heating and cooking, meaning that coal and wood are not burned in stoves inside the home. However, Alexandra has a high density of informal food vendors that cook almost exclusively over open flames, using inefficient three-stone fires which emit large concentrations of particulates. Vendors start cooking in the early morning and continue throughout the day and into the evening, resulting in a diurnal PM profile which does display moderate concentration enhancements in morning and evening, but with elevated PM concentrations during midday as well. Bodibeng is a more extreme and localized example of the impact of informal commercial food service on PM concentrations. The Bodibeng monitoring site is located immediately adjacent to a major taxi rank, where hundreds of taxis congregate during the hours of roughly 10.00 a.m. and 3.00 p.m. LT, between commute times and when the majority of taxi riders are at work. During these hours, informal food vendors cook meals for taxi drivers almost exclusively over open flames. The result is a tertiary PM peak in Bod-

ibeng data between the hours of 10.00 a.m. and 3.00 p.m. LT associated with informal commercial activity.

3.4 Satellite data as a proxy for air quality

As discussed above, while there is a trend of using remotely sensed data as a proxy for air quality at the ground, it is necessary to evaluate the appropriateness of this practice in each individual area. Figure 12 displays month-averaged PM_{10} and $PM_{2.5}$ concentrations from ground monitoring sites throughout Gauteng, plotted against month-averaged satellite parameters (AOD, α and UVAI) for the Gauteng satellite grid box. Solid lines represent least-squares linear regression fits, considered separately for each ground monitoring site type. R^2 values for linear regressions are annotated on the figure. Poor correlation is immediately evident between PM concentrations and both AOD and UVAI. Further, what correlation does exist is the opposite of what is expected – since AOD and UVAI both capture an overall light extinction due to particles, one would expect elevated PM concentration to correspond with elevated AOD and UVAI. However, the highest PM concentrations occur at the ground during winter months, when AOD and UVAI are at a minimum, while the maxima in AOD and UVAI tend to occur during spring and into the summer, when deeper boundary layers and an absence of domestic burning result PM concentration minima. The correlation between PM concentration and α is relatively good (except in industrial areas), with low α (larger particles in the column) corresponding to higher concentrations at the ground. We suggest that this correlation is coincidental, however, with higher concentrations at the ground corresponding to domestic burning and occurring in winter, when larger dust particles appear to be more prevalent in the column.

There are a number of reasons for the discrepancy between ground and satellite data in metropolitan areas of South Africa. First, there is strong potential for vertical inhomogeneity to result in a disconnect between column and ground aerosol properties. For example, Campbell et al. (2003) and Chand et al. (2009) indicated that biomass burning emissions from fires in the tropics and subtropics tend to be transported to

South Africa in stratified layers aloft. Further, Tyson et al. (1996) found that there are frequent, persistent absolutely stable layers at 3 and 5 km above much of South Africa, increasing the potential for stratified plumes of pollutants above the ground. While concentrated plumes of particles in stratified layers above the ground would impact column aerosol properties, they would not affect ground concentrations of particulates unless atmospheric instability caused those particles to be vertically mixed into the planetary boundary layer and to the surface. Therefore, characteristics of column aerosol properties are not necessarily indicative of any trends in ground PM concentrations – particularly in South Africa's stratified atmosphere. Next, the highest concentrations of particulates in South Africa are observed in winter, when domestic burning emissions are released into an extremely shallow boundary layer, often on the order of 50 m or less (Tyson et al., 1996). Because these emissions are confined in a layer so close to the ground, it is unlikely that satellite retrievals are able to resolve the difference between the concentrated aerosol layer and the ground itself. Third is the issue of temporal resolution. Figure 13 shows average wintertime PM_{10} and $PM_{2.5}$ diurnal profiles for each site type, with shaded boxes representing the time window in which Terra, MISR, and Aqua satellites pass over South Africa. Terra and MISR (09:00 to 11:00 LT) tend to pass over South Africa on the tail end of enhanced PM concentrations from morning domestic burning, while Aqua's pass over time (13:00–15:00 LT) coincides with the minimum PM concentrations of the day. While PM concentrations tend to be elevated throughout the day in all sites during winter, the average daily, weekly, and winter PM concentrations at the ground are strongly influenced by morning and evening maxima that are not observed by satellites. Therefore, the discrepancy between satellite passover times and elevated PM concentrations indicates that remotely sensed data are unlikely to capture the trend of significantly enhanced PM concentration at the ground. Finally, spatial resolution is a factor prohibiting satellite data from appropriately representing ground PM concentrations. PM concentrations between township, suburban, and industrial sites just a few km apart are significantly different (Fig. 10), underscoring the significant local variability in PM concentrations resulting from unique

Title Page

Abstract   Introduction

Conclusions   References

Tables   Figures

◄   ►

◄   ►

Back   Close

Full Screen / Esc

Printer-friendly Version

Interactive Discussion

source density in each area. Satellite measures of aerosol properties must be averaged over spatial scales on the order of 1° × 1°, which includes many areas with low overall concentrations and areas (e.g. urban/suburban residential and industrial in Fig. 11) where the discrepancy between seasonal profiles of PM do not vary significantly in magnitude. The problem of extreme PM concentrations at the ground appears to be a highly localized one impacting primarily low-income areas of South Africa, and the vertical integration, low time resolution, and spatial averaging required with satellite data precludes their use in understanding and predicting ground PM characteristics.

4 Conclusions

Here we present a comprehensive study of air quality in South Africa's metropolitan centers, based on decadal averages of remotely sensed aerosol column data and multi-year averages from ground-based air quality sampling sites. Aerosol climatology from satellite platforms was based on AOD, Ängström exponent and UVAI, and GOCART model results were also analyzed. AOD was found to reach a maximum of 0.12–0.20 in late winter and early spring (ASO), corresponding with elevated column concentrations of absorbing aerosol from close-proximity fires in Mozambique, Zimbabwe, and eastern South Africa, as well as from enhanced windblown dust generation during dry and windy months. Minimum AOD of 0.05–0.10 occurs during winter, when domestic burning emissions are highest and air quality at the ground is worst, suggesting that this aerosol is confined to a very shallow layer and does not impact overall column aerosol characteristics despite its importance at the surface. AOD in metropolitan areas of South Africa is a factor of 3–6 lower than reported for megacities worldwide, and is lower than previously reported in the rural northeast part of the country that is closer in proximity to biomass burning sources. Ängström exponent reaches a maximum of 1.0–1.8 in spring and summer at sites closest to biomass burning sources, reflecting the importance of regional fires as sources of small particles. Ängström reaches a minimum of 0.6–1.0 in winter, when dry conditions appear to result in an enhanced

Title Page

Abstract | Introduction

Conclusions | References

Tables | Figures

|◄ | ►|

◄ | ►

Back | Close

Full Screen / Esc

Printer-friendly Version

Interactive Discussion

contribution of coarse dust particles to column aerosol. Ängström exponent is highly correlated with CWV and is markedly lower at continental sites, suggesting that coarse dust particles contribute significantly to total column aerosol in inland South Africa. UVAI reaches a maximum of 1.0–1.2 in spring and summer, coinciding with the pres-
5 ence of strongly-absorbing dust and biomass burning particles, and is at a minimum of 0.7 in winter, when dust aerosols appear to contribute a larger fraction of column aerosol but integrated column concentrations are very low. Satellite results in Cape Town are significantly different than other sites, reflecting a difference between clean marine vs. polluted continental airmass origins. The Gauteng and industrial Highveld
10 areas of South Africa have been identified as one of the world's polluted megacities based on NO_2 concentrations. However, satellite data suggest that the area is not a major regional source of particulates. Overall, satellite data provide a good representation of large-scale, regional, and seasonal trends in column particulates across South Africa.
15 Ground air quality results are based on PM data from 19 sites in Gauteng province, which is the most significant population and industrial center of South Africa. Ground monitoring sites fall into 4 categories: township areas with close proximity domestic burning, urban/suburban residential areas, industrial areas, and traffic sites directly adjacent to major on-road sources. Based on monthly averages, townships experience 51
20 and 78 % higher PM_{10} concentrations than urban/suburban residential and industrial areas, respectively, quantitatively confirming previous studies indicating that the poorest air quality in South Africa is found in low-income areas. Both PM_{10} and $PM_{2.5}$ reach distinct maxima in winter (June, July, or August) in all non-industrial sites, while two maxima are observed in industrial sites and correspond to photochemical particulate
25 production and deeper, unstable boundary layers in summer and domestic burning in winter. Both PM_{10} and $PM_{2.5}$ display diurnal patterns, with elevated concentration in the morning (06:00–09:00 LT) and maximum concentration in the evening (17:00–22:00 LT) in all seasons. These diurnal profiles are especially distinct during winter in low-income areas, with evening PM_{10} and $PM_{2.5}$ on average reaching 203 and 105 $\mu g\,m^{-3}$, respec-

tively. Monthly and diurnal PM concentrations at the ground vary significantly between sites just a few km apart, underscoring the importance of source strength and density in determining particulate air quality at a highly localized level. This result also indicates that a "typical" low income area is difficult to define solely in terms of the magnitude of particulate concentrations.

If satellite measurements of column aerosol properties were an appropriate proxy for air quality at the ground in urban South Africa, one would expect AOD to be positively correlated with PM_{10} and $PM_{2.5}$ concentrations. This, however, is not observed, as correlations between AOD and PM are weak and negative. PM_{10} is negatively correlated with α, suggesting that higher ground PM concentrations are associated with larger particles in the column. We suggest, however, that this correlation is coincidental due to seasonal variation in which high wintertime PM concentrations at the ground occur during the dry season when coarse dust particles contribute an elevated fraction of column aerosol. Other satellite and model products show little correlation with ground PM concentrations, and it appears as though satellites are unable to resolve even extremely high PM concentrations at the ground during winter in South Africa. This discrepancy is likely the result of a combination of atmospheric dynamics (absolutely stable layers aloft, concentrated pollutants transported aloft, and high wintertime PM confined within a very shallow boundary layer) and time and spatial resolution (satellites pass over southern Africa during off-peak times for PM concentration, and data must be averaged over large areas).

The inability of satellites to capture trends in ground PM concentrations in South Africa indicates that monitoring and characterization of air quality in South Africa will require extensive networks of ground monitoring stations producing quality data across the country, as well as intensive multi-platform campaigns aimed at understanding the relationship between ground and remotely-sensed air quality data. Further advances in understanding would follow regular monitoring of vertical profiles of criteria pollutants. South Africa's current monitoring networks are in varying states of functionality and management, meaning that many air quality data time series are either incomplete or

Title Page

Abstract | Introduction

Conclusions | References

Tables | Figures

|◄ | ►|

◄ | ►

Back | Close

Full Screen / Esc

Printer-friendly Version

Interactive Discussion

poor in quality. Data are controlled individually by each network, so a study like this one requires many different official requests, approvals, and waiting times for data. Further, these monitoring sites tend to be in urban and industrial centers of South Africa like those considered in this work. However, roughly 40 % of South Africa's population resides in rural settlements, and little is known about air quality in these areas. Based on results presented here, we suggest that a systematic effort be made in South Africa to improve and centralize management, data quality, and data availability amongst existing ground monitoring networks, in addition to an expansion of ground monitoring sites into rural areas.

References

Abdou, W. A., Diner, D. J., Martonchik, J. V., Bruegge, C. J., Kahn, R. A., Gaitley, B. J., Crean, K. A., Remer, L. A., and Holben, B.: Comparison of coincident Multiangle Imaging Spectroradiometer and Moderate Resolution Imaging Spectroradiometer aerosol optical depths over land and ocean scenes containing Aerosol Robotic Network sites, J. Geophys. Res.-Atmos., 110, 8497, doi:10.1029/2004JD004693, 2005. 24712

Alam, K., Qureshi, S., and Blaschke, T.: Monitoring spatio-temporal aerosol patterns over Pakistan based on MODIS, TOMS and MISR satellite data and a HYSPLIT model, Atmos. Environ., 45, 4641–4651, doi:10.1016/j.atmosenv.2011.05.055, 2011. 24705

Beirle, S., Platt, U., Wenig, M., and Wagner, T.: Highly resolved global distribution of tropospheric NO_2 using GOME narrow swath mode data, Atmos. Chem. Phys., 4, 1913–1924, doi:10.5194/acp-4-1913-2004, 2004. 24716

Bigala, T. A.: Aerosol loading over the South African Highveld, Ph. D. thesis, University of Witswatersrand, Johannesburg, South Africa, 2009. 24714

Campbell, J. R., Welton, E. J., Spinhirne, J. D., Ji, Q., Tsay, S.-C., Piketh, S. J., Barenbrug, M., and Holben, B. N.: Micropulse lidar observations of tropospheric aerosols over northeastern South Africa during the ARREX and SAFARI 2000 dry season experiments, J. Geophys. Res., 108, D10S07, doi:10.1029/2002JD002563, 2003. 24705, 24706, 24713, 24714, 24724

Carmona, I. and Alpert, P.: Synoptic classification of moderate resolution imaging spectroradiometer aerosols over Israel, J. Geophys. Res.-Atmos., 114, D07208, doi:10.1029/2008JD010160, 2009. 24705

Chand, D., Wood, R., Anderson, T., Satheesh, S., and Charlson, R.: Satellite-derived direct radiative effect of aerosols dependent on cloud cover, Nat. Geosci., 2, 181–184, 2009. 24706, 24724

Chin, M., Ginoux, P., Kinne, S., Torres, O., Holben, B. N., Duncan, B. N., Martin, R. V., Logan, J. A., Higurashi, A., and Nakajima, T.: Tropospheric aerosol optical thickness from the GOCART model and comparisons with satellite and sun photometer measurements, J. Atmos. Sci., 59, 461–483, doi:10.1175/1520-0469(2002)059<0461:TAOTFT>2.0.CO;2, 2002. 24708, 24719

Chu, D. A., Kaufman, Y. J., Ichoku, C., Remer, L. A., Tanra, D., and Holben, B. N.: Validation of MODIS aerosol optical depth retrieval over land, Geophys. Res. Lett., 29, MOD2-1–MOD2-4, doi:10.1029/2001GL013205, 2002. 24713

Cooke, W. F. and Wilson, J. J.: A global black carbon aerosol model, J. Geophys. Res.-Atmos., 101, 19395–19409, 1996. 24705

Crosbie, E., Sorooshian, A., Monfared, N. A., Shingler, T., and Esmaili, O.: A multi-year aerosol characterization for the greater Tehran area using satellite, surface, and modeling data, Atmosphere, 5, 178–197, doi:10.3390/atmos5020178, 2014. 24705

Diner, D. J., Abdou, W. A., Ackerman, T. P., Crean, K., Gordon, H. R., Kahn, R. A., Martonchik, J. V., McMuldroch, S., Paradise, S. R., Pinty, B., Verstraete, M. M., Wang, M., and West, R. A.: Level 2 aerosol retrieval algorithm theoretical basis, Jet Propulsion Laboratory, California Institute of Technology, 2001a. 24707

South African aerosol

S. P. Hersey et al.

Title Page

Abstract | Introduction

Conclusions | References

Tables | Figures

Back | Close

Full Screen / Esc

Printer-friendly Version

Interactive Discussion

Diner, D. J., Abdou, W. A., Bruegge, C. J., Conel, J. E., Crean, K. A., Gaitley, B. J., Helm-linger, M. C., Kahn, R. A., Martonchik, J. V., Pilorz, S. H., and Holben, B. N.: MISR aerosol optical depth retrievals over southern Africa during the SAFARI – 2000 Dry Season Campaign, Geophys. Res. Lett., 28, 3127, doi:10.1029/2001GL013188, 2001b. 24707

Draxler, R. R. and Rolph, G.: HYSPLIT (HYbrid Single-Particle Lagrangian Integrated Trajectory) model access via NOAA ARL READY website, available at: http://www.arl.noaa.gov/ready/hysplit4.html (last access: 4 May 2014), NOAA Air Resources Laboratory, Silver Spring, 2003. 24709

Eck, T. F., Holben, B. N., Ward, D. E., Mukelabai, M. M., Dubovik, O., Smirnov, A., Schafer, J. S., Hsu, N. C., Piketh, S. J., Queface, A., Roux, J. L., Swap, R. J., and Slutsker, I.: Variability of biomass burning aerosol optical characteristics in southern Africa during the SAFARI 2000 dry season campaign and a comparison of single scattering albedo estimates from radiometric measurements, J. Geophys. Res., 108, 8477, doi:10.1029/2002JD002321, 2003. 24705, 24713, 24714, 24715, 24717, 24718

Engelbrecht, J. P., Swanepoel, L., Zunckel, M., Chow, J. C., Watson, J. G., and Egami, R. T.: Modelling PM_{10} aerosol data from the Qalabotjha low-smoke fuels macro-scale experiment in South Africa, Ecol. Model., 127, 235–244, 2000. 24704, 24706, 24714

Engelbrecht, J. P., Swanepoel, L., Chow, J. C., Watson, J. G., and Egami, R. T.: $PM_{2.5}$ and PM_{10} concentrations from the Qalabotjha low-smoke fuels macro-scale experiment in South Africa, Environ. Monit. Assess., 69, 1–15, 2001. 24704, 24706, 24714

Engelbrecht, J. P., Swanepoel, L., Chow, J. C., Watson, J. G., and Egami, R. T.: The comparison of source contributions from residential coal and low-smoke fuels, using CMB modeling, in South Africa, Environ. Sci. Policy, 5, 157–167, 2002. 24704, 24706, 24714

Formenti, P., Winkler, H., Fourie, P., Piketh, S., Makgopa, B., Helas, G., and Andreae, M. O.: Aerosol optical depth over a remote semi-arid region of South Africa from spectral measurements of the daytime solar extinction and the nighttime stellar extinction, Atmos. Res., 62, 11–32, doi:10.1016/S0169-8095(02)00021-2, 2002. 24705, 24713, 24714

Formenti, P., Elbert, W., Maenhaut, W., Haywood, J., Osborne, S., and Andreae, M. O.: Inorganic and carbonaceous aerosols during the Southern African Regional Science Initiative (SAFARI 2000) experiment: chemical characteristics, physical properties, and emission data for smoke from African biomass burning, J. Geophys. Res., 108, 8488, doi:10.1029/2002JD002408, 2003. 24705, 24713, 24717

South African aerosol

S. P. Hersey et al.

Title Page

Abstract	Introduction
Conclusions	References
Tables	Figures

|◀ | ▶|

◀ | ▶

Back | Close

Full Screen / Esc

Printer-friendly Version

Interactive Discussion

FRIDGE: Study to examine the potential socio-economic impact of measures to reduce air pollution from combustion. Part 1 report: Definition of air pollutants associated with combustion processes., Tech. rep., Airshed Planning Professionals/Bentley West Management Consultants report to the Trade and Industry Chamber/Fund for Research into Industrial Development, Growth and Equity (FRIDGE), Johannesburg, 2004. 24704

Guo, J.-P., Zhang, X.-Y., Wu, Y.-R., Zhaxi, Y., Che, H.-Z., La, B., Wang, W., and Li, X.-W.: Spatio-temporal variation trends of satellite-based aerosol optical depth in China during 1980–2008, Atmos. Environ., 45, 6802–6811, 2011. 24705

Herman, J., Bhartia, P., Torres, O., Hsu, C., Seftor, C., and Celarier, E.: Global distribution of UV-absorbing aerosols from Nimbus 7/TOMS data, J. Geophys. Res.-Atmos., 102, 16911–16922, 1997. 24707

Hirsikko, A., Vakkari, V., Tiitta, P., Manninen, H. E., Gagné, S., Laakso, H., Kulmala, M., Mirme, A., Mirme, S., Mabaso, D., Beukes, J. P., and Laakso, L.: Characterisation of sub-micron particle number concentrations and formation events in the western Bushveld Igneous Complex, South Africa, Atmos. Chem. Phys., 12, 3951–3967, doi:10.5194/acp-12-3951-2012, 2012. 24717

Hsu, N., Herman, J., Bhartia, P., Seftor, C., Torres, O., Thompson, A., Gleason, J., Eck, T., and Holben, B.: Detection of biomass burning smoke from TOMS measurements, Geophys. Res. Lett., 23, 745–748, 1996. 24719

Hsu, N. C., Tsay, S.-C., King, M. D., and Herman, J. R.: Aerosol properties over bright-reflecting source regions, IEEE T. Geosci. Remote, 42, 557–569, 2004. 24708

Hsu, N. C., Tsay, S.-C., King, M. D., and Herman, J. R.: Deep blue retrievals of Asian aerosol properties during ACE-Asia, IEEE T. Geosci. Remote, 44, 3180–3195, 2006. 24708

Kahn, R. A., Garay, M. J., Nelson, D. L., Yau, K. K., Bull, M. A., Gaitley, B. J., Martonchik, J. V., and Levy, R. C.: Satellite-derived aerosol optical depth over dark water from MISR and MODIS: comparisons with AERONET and implications for climatological studies, J. Geophys. Res.-Atmos., 112, D18205, doi:10.1029/2006JD008175, 2007. 24712, 24713

Kaskaoutis, D., Kosmopoulos, P., Kambezidis, H., and Nastos, P.: Aerosol climatology and discrimination of different types over Athens, Greece, based on MODIS data, Atmos. Environ., 41, 7315–7329, 2007. 24705

Kumar, K. R., Sivakumar, V., Reddy, R., Gopal, K. R., and Adesina, A. J.: Inferring wavelength dependence of AOD and Ångström exponent over a sub-tropical station in South Africa using AERONET data: Influence of meteorology, long-range transport and curvature effect,

Sci. Total Environ., 461, 397–408, doi:10.1016/j.scitotenv.2013.04.095, 2013. 24705, 24706, 24715, 24718

LeCanut, P., Andreae, M., Harris, G., Wienhold, F., and Zenker, T.: Airborne studies of emissions from savanna fires in southern Africa, 1. Aerosol emissions measured with a laser optical particle counter, J. Geophys. Res., 101, 23615–23630, 1996. 24714, 24719

Levy, R. C., Remer, L. A., Kleidman, R. G., Mattoo, S., Ichoku, C., Kahn, R., and Eck, T. F.: Global evaluation of the Collection 5 MODIS dark-target aerosol products over land, Atmos. Chem. Phys., 10, 10399–10420, doi:10.5194/acp-10-10399-2010, 2010. 24717

Lourens, A. S. M.: Air quality in the Johannesburg-Pretoria megacity: its regional influence and identification of parameters that could mitigate pollution/ASM Lourens, Ph. D. thesis, North-West University, Potchefstroom, South Africa, 2012. 24716

Luo, Y., Zheng, X., and Chen, J.: A climatology of aerosol optical depth over China from recent 10 years of MODIS remote sensing data, Int. J. Climatol., 34, 863–870, doi:10.1002/joc.3728, 2014. 24705, 24716

Magi, B. I., Ginoux, P., Ming, Y., and Ramaswamy, V.: Evaluation of tropical and extratropical Southern Hemisphere African aerosol properties simulated by a climate model, J. Geophys. Res., 114, D14204, doi:10.1029/2008JD011128, 2009. 24706, 24713, 24714

Marey, H. S., Gille, J. C., El-Askary, H. M., Shalaby, E. A., and El-Raey, M. E.: Aerosol climatology over Nile Delta based on MODIS, MISR and OMI satellite data, Atmos. Chem. Phys., 11, 10637–10648, doi:10.5194/acp-11-10637-2011, 2011. 24705

Massie, S. T., Gille, J. C., Edwards, D. P., and Nandi, S.: Satellite observations of aerosol and {CO} over Mexico City, Atmos. Environ., 40, 6019–6031, 2006. 24705, 24716

Mdluli, T. N.: The societal dimensions of domestic coal combustion: people's perceptions and indoor aerosol monitoring, Ph.D. thesis, University of the Witwatersrand, Johannesburg, South Africa, 2007. 24714

Pauw, C., Friedl, A., Holm, D., and John, J., Kornelius, G., Oosthuisen, R., and van Niekerk, A.: Report to the Royal Danish Embassy and the Department of Environmental Affairs and Tourism: air pollution in dense, low-income settlements in South Africa, issue I., Tech. rep., NOVA Institute, Pretoria, South Africa, 2008. 24704, 24714

Piketh, S. J., Annegarn, H. J., and Tyson, P. D.: Lower tropospheric aerosol loadings over South Africa: the relative contribution of aeolian dust, industrial emissions, and biomass burning, J. Geophys. Res., 104, 1597–1607, doi:10.1029/1998JD100014, 1999. 24713, 24717, 24720

Title Page

Abstract | Introduction

Conclusions | References

Tables | Figures

|◀ | ▶|

◀ | ▶

Back | Close

Full Screen / Esc

Printer-friendly Version

Interactive Discussion

Piketh, S. J., Swap, R. J., Maenhaut, W., Annegarn, H. J., and Formenti, P.: Chemical evidence of long-range atmospheric transport over southern Africa, J. Geophys. Res., 107, 4817, doi:10.1029/2002JD002056, 2002. 24705, 24713, 24720

Qi, Y., Ge, J., and Huang, J.: Spatial and temporal distribution of MODIS and MISR aerosol optical depth over northern China and comparison with AERONET, Chinese Sci. Bull., 58, 2497–2506, 2013. 24705, 24718

Queface, A. J., Piketh, S. J., Eck, T. F., Tsay, S.-C., and Mavume, A. F.: Climatology of aerosol optical properties in Southern Africa, Atmos. Environ., 45, 2910–2921, doi:10.1016/j.atmosenv.2011.01.056, 2011. 24706, 24713, 24714, 24715

Remer, L. A., Kaufman, Y., Tanré, D., Mattoo, S., Chu, D., Martins, J. V., Li, R.-R., Ichoku, C., Levy, R., Kleidman, R., Eck, T. F., Vermote, E., and Holben, B. N.: The MODIS aerosol algorithm, products, and validation, J. Atmos. Sci., 62, 947–973, doi:10.1175/JAS3385.1, 2005. 24707, 24717

Rienecker, M. M., Suarez, M. J., Gelaro, R., Todling, R., Bacmeister, J., Liu, E., Bosilovich, M. G., Schubert, S. D., Takacs, L., Kim, G.-K., Bloom, S., Chen, J., Collins, D., Conaty, A., da Silva, A., Gu, W., Joiner, J., Koster, R. D., Lucchesi, R., Molod, A., Owens, T., Pawson, S., Pegion, P., Redder, C. R., Reichle, R., Robertson, F. R., Ruddick, A. G., Sienkiewicz, M., and Woollen, J.: MERRA: NASA's Modern-Era Retrospective Analysis for Research and Applications, J. Climate, 24, 3624–3648, doi:10.1175/JCLI-D-11-00015.1, 2011. 24715

Robles-Gonzalez, C. and de Leeuw, G.: Aerosol properties over the SAFARI2000 area retrieved from ATSR-2, J. Geophys. Res., 113, D05206, doi:10.1029/2007JD008636, 2008. 24718

Ross, K. E., Piketh, S. J., Bruintjes, R. T., Burger, R. P., Swap, R. J., and Annegarn, H. J.: Spatial and seasonal variations in CCN distribution and the aerosol-CCN relationship over southern Africa, J. Geophys. Res., 108, 8481, doi:10.1029/2002JD002384, 2003. 24706, 24713, 24714

Singh, R., Dey, S., Tripathi, S., Tare, V., and Holben, B.: Variability of aerosol parameters over Kanpur, northern India, J. Geophys. Res.-Atmos., 109, D23206, doi:10.1029/2004JD004966, 2004. 24705

Sorooshian, A., Wonaschütz, A., Jarjour, E. G., Hashimoto, B. I., Schichtel, B. A., and Betterton, E. A.: An aerosol climatology for a rapidly growing arid region (southern Arizona): major aerosol species and remotely sensed aerosol properties, J. Geophys. Res.-Atmos., 116, D19205, doi:10.1029/2011JD016197, 2011. 24705

South African aerosol

S. P. Hersey et al.

Title Page

Abstract	Introduction
Conclusions	References
Tables	Figures

| |◄ | ►| |
| ◄ | ► |

| Back | Close |

Full Screen / Esc

Printer-friendly Version

Interactive Discussion

Sreekanth, V. and Kulkarni, P.: Spatio-temporal variations in columnar aerosol optical properties over Bay of Bengal: signatures of elevated dust, Atmos. Environ., 69, 249–257, 2013. 24705

Tesfaye, M., Sivakumar, V., Botai, J., and Tsidu, G. M.: Aerosol climatology over South Africa based on 10 years of Multiangle Imaging Spectroradiometer (MISR) data, J. Geophys. Res., 116, D20216, doi:10.1029/2011JD016023, 2011. 24705, 24706, 24707, 24715

Tiitta, P., Vakkari, V., Croteau, P., Beukes, J. P., van Zyl, P. G., Josipovic, M., Venter, A. D., Jaars, K., Pienaar, J. J., Ng, N. L., Canagaratna, M. R., Jayne, J. T., Kerminen, V.-M., Kokkola, H., Kulmala, M., Laaksonen, A., Worsnop, D. R., and Laakso, L.: Chemical composition, main sources and temporal variability of PM_1 aerosols in southern African grassland, Atmos. Chem. Phys., 14, 1909–1927, doi:10.5194/acp-14-1909-2014, 2014. 24705

Tyson, P. D., Garstang, M., Swap, R., Kållberg, P., and Edwards, M.: An air transport climatology for Subtropical Southern Africa, Int. J. Climatol., 16, 265–291, doi:10.1002/(SICI)1097-0088(199603)16:3<265::AID-JOC8>3.3.CO;2-D, 1996. 24725

Venter, A. D., Vakkari, V., Beukes, J. P., Van Zyl, P. G., Laakso, H., Mabaso, D., Tiitta, P., Josipovic, M., Kulmala, M., Pienaar, J. J. and Laakso, L.: An air quality assessment in the industrialised western Bushveld Igneous Complex, South Africa, S. Afr. J. Sci., 108, 1–10, 2012. 24714

von Schirnding, Y., Bruce, N., Smith, K., Ballard-Tremeer, G., Ezzati, M., and Lvovsky, K.: Addressing the impact of household energy and indoor air pollution on the health of the poor: implications for policy action and intervention measures., Tech. rep., World Health Organization (WHO) Commission on Macroeconomics and Health working group 5: improving health outcomes of the poor, Geneva, 2002. 24704

Wichmann, J. and Voyi, K. V.: Air pollution epidemiological studies in South Africa: need for freshening up, Rev. Environ. Health, 20, 265–302, 2005. 24704

Winkler, H.: Energy policies for sustainable development in South Africa, Energ. Sust. Develop., 11, 26–34, doi:10.1016/S0973-0826(08)60561-X, 2007. 24714

Winkler, H., Formenti, P., Esterhuyse, D. J., Swap, R. J., Helas, G., Annegarn, H. J., and Andreae, M. O.: Evidence for large-scale transport of biomass burning aerosols from sunphotometry at a remote South African site, Atmos. Environ., 42, 5569–5578, doi:10.1016/j.atmosenv.2008.03.031, 2008. 24706, 24713, 24714

Yeh, E.: Indoor air pollution in developing countries: Household use of traditional biomass fuels and the impact on mortality, University of California, Berkeley, 2004. 24704

Title Page

Abstract | Introduction

Conclusions | References

Tables | Figures

|◀ | ▶|

◀ | ▶

Back | Close

Full Screen / Esc

Printer-friendly Version

Interactive Discussion

Zhang, Z., Wenig, M., Zhou, W., Diehl, T., Chan, K.-L., and Wang, L.: The contribution of different aerosol sources to the Aerosol Optical Depth in Hong Kong, Atmos. Environ., 83, 145–154, doi:10.1016/j.atmosenv.2013.10.047, 2014. 24705, 24716

Zhuang, B., Wang, T., Li, S., Liu, J., Talbot, R., Mao, H., Yang, X., Fu, C., Yin, C., Zhu, J., Che, H., and Zhang, X.: Optical properties and radiative forcing of urban aerosols in Nanjing, China, Atmos. Environ., 83, 43–52, doi:10.1016/j.atmosenv.2013.10.052, 2014. 24705, 24716, 24718

South African aerosol

S. P. Hersey et al.

Title Page

Abstract | Introduction

Conclusions | References

Tables | Figures

|◄ | ►|

◄ | ►

Back | Close

Full Screen / Esc

Printer-friendly Version

Interactive Discussion

Table 1. Ground-based air quality monitoring sites in the Gauteng area.

Site	Network	Type	Data	Date Range
Alexandra	Joburg	Township/Domestic Burning	PM_{10}	1 Jan 2004 to 31 Oct 2010
Jabavu (Soweto)	Joburg	Township/Domestic Burning	PM_{10}	14 Jul 2004 to 20 May 2011
Orange Farm	Joburg	Township/Domestic Burning	PM_{10}	17 May 2004 to 1 Jun 2011
Delta Park	Joburg	Urban/Suburban Residential	PM_{10}	31 Jul 2004 to 09 Dec 2010
Newtown	Joburg	Urban/Suburban Residential	PM_{10}	31 Jul 2004 to 1 Jun 2011
Buccleuch	Joburg	Traffic	PM_{10}, $PM_{2.5}$	31 Jul 2004 to 1 Jun 2011
Bodibeng	Tshwane	Township/Domestic Burning	PM_{10}	1 May 2012 to 28 Feb 2014
Olivienhoutbosch	Tshwane	Township/Domestic Burning	PM_{10}	1 May 2012 to 31 Dec 2013
PTA West	Tshwane	Industrial	PM_{10}	25 Jun 2012 to 5 Oct 2014
Rosslyn	Tshwane	Industrial	PM_{10}	20 Jun 2012 to 06 Mar 2014
Ekandustria	Tshwane	Industrial	PM_{10}	1 Sep 2012 to 21 Feb 2014
Booysens	Tshwane	Urban/Suburban Residential	PM_{10}	1 May 2012 to 28 Feb 2014
Etwatwa	Ekurhuleni	Township/Domestic Burning	PM_{10}	1 Jan 2011 to 30 Sep 2012
Tembisa	Ekurhuleni	Township/Domestic Burning	PM_{10}	1 Jul 2011 to 30 Sep 2011
Diepkloof	VTAPA	Township/Domestic Burning	PM_{10}, $PM_{2.5}$	1 Feb 2007 to 31 Dec 2012
Sebokeng	VTAPA	Township/Domestic Burning	PM_{10}, $PM_{2.5}$	1 Feb 2007 to 31 Dec 2012
Sharpeville	VTAPA	Township/Domestic Burning	PM_{10}, $PM_{2.5}$	1 Mar 2007 to 31 Dec 2012
Zamdela	VTAPA	Township/Domestic Burning	PM_{10}, $PM_{2.5}$	1 Mar 2007 to 31 Dec 2012
Three Rivers	VTAPA	Industrial	PM_{10}, $PM_{2.5}$	1 Feb 2007 to 31 Dec 2012

Table 2. Seasonal averages of satellite data from the Aqua, Terra, and MISR platforms for each region and as a South Africa average, for the period 1 January 2000 to 31 Dececember 2009.

Parameter	Region	Platform	Summer	Fall	Winter	Spring
AOD	CPT	Aqua	0.07 ± 0.01	0.06 ± 0.02	0.05 ± 0.01	0.19 ± 0.02
		Terra	0.08 ± 0.02	0.06 ± 0.02	0.06 ± 0.01	0.13 ± 0.01
		MISR	0.11 ± 0.13	0.13 ± 0.18	0.10 ± 0.03	0.14 ± 0.05
		Average	0.09 ± 0.08	0.08 ± 0.10	0.07 ± 0.02	0.15 ± 0.03
	Bloem	Aqua	0.10 ± 0.03	0.08 ± 0.03	0.10 ± 0.02	0.12 ± 0.05
		Terra	0.09 ± 0.02	0.09 ± 0.03	0.10 ± 0.03	0.13 ± 0.03
		MISR	0.13 ± 0.03	0.09 ± 0.03	0.08 ± 0.04	0.16 ± 0.05
		Average	0.11 ± 0.03	0.09 ± 0.03	0.09 ± 0.03	0.14 ± 0.04
	Joburg/PTA	Aqua	0.13 ± 0.04	0.13 ± 0.02	0.12 ± 0.04	0.17 ± 0.06
		Terra	0.15 ± 0.04	0.14 ± 0.02	0.12 ± 0.03	0.17 ± 0.03
		MISR	0.18 ± 0.05	0.12 ± 0.02	0.12 ± 0.04	0.21 ± 0.05
		Average	0.15 ± 0.04	0.13 ± 0.02	0.12 ± 0.04	0.18 ± 0.05
	HVAPA	Aqua	0.15 ± 0.04	0.12 ± 0.03	0.11 ± 0.03	0.19 ± 0.06
		Terra	0.08 ± 0.03	0.08 ± 0.03	0.10 ± 0.02	0.13 ± 0.03
		MISR	0.12 ± 0.04	0.08 ± 0.02	0.08 ± 0.03	0.14 ± 0.05
		Average	0.12 ± 0.04	0.09 ± 0.03	0.10 ± 0.03	0.15 ± 0.05
	Durban	Aqua	0.09 ± 0.02	0.09 ± 0.02	0.13 ± 0.03	0.14 ± 0.03
		Terra	0.09 ± 0.02	0.09 ± 0.02	0.13 ± 0.03	0.15 ± 0.03
		MISR	0.18 ± 0.09	0.13 ± 0.05	0.18 ± 0.05	0.24 ± 0.08
		Average	0.12 ± 0.06	0.11 ± 0.03	0.15 ± 0.04	0.18 ± 0.05
	South Africa	Average	0.12 ± 0.05	0.10 ± 0.05	0.11 ± 0.03	0.16 ± 0.05
α	CPT	Aqua	1.19 ± 0.09	1.26 ± 0.11	1.21 ± 0.12	1.39 ± 0.10
		Terra	1.25 ± 0.12	1.39 ± 0.14	1.40 ± 0.13	0.97 ± 0.09
		Average	1.22 ± 0.10	1.33 ± 0.12	1.31 ± 0.13	1.18 ± 0.09
	Bloem	Aqua	1.18 ± 0.32	0.90 ± 0.20	0.67 ± 0.06	0.92 ± 0.22
		Terra	0.99 ± 0.34	0.82 ± 0.19	0.70 ± 0.11	0.92 ± 0.30
		Average	1.09 ± 0.33	0.86 ± 0.19	0.69 ± 0.09	0.92 ± 0.26
	Joburg/PTA	Aqua	1.26 ± 0.28	0.86 ± 0.12	0.69 ± 0.08	0.95 ± 0.29
		Terra	1.20 ± 0.22	0.88 ± 0.15	0.80 ± 0.19	1.16 ± 0.34
		Average	1.23 ± 0.25	0.87 ± 0.13	0.75 ± 0.15	1.06 ± 0.31
	HVAPA	Aqua	1.13 ± 0.35	0.95 ± 0.25	0.69 ± 0.07	0.97 ± 0.27
		Terra	1.22 ± 0.23	0.79 ± 0.19	0.71 ± 0.08	1.39 ± 0.24
		Average	1.18 ± 0.30	0.87 ± 0.22	0.70 ± 0.08	1.18 ± 0.25
	Durban	Aqua	1.50 ± 0.13	1.33 ± 0.10	1.09 ± 0.11	1.68 ± 0.11
		Terra	1.40 ± 0.12	1.29 ± 0.11	1.08 ± 0.15	1.61 ± 0.10
		Average	1.45 ± 0.13	1.31 ± 0.11	1.09 ± 0.13	1.65 ± 0.11
	South Africa	Average	1.23 ± 0.24	1.05 ± 0.16	0.90 ± 0.12	1.20 ± 0.23
UVAI		CPT	1.09 ± 0.28	0.73 ± 0.10	0.74 ± 0.09	0.95 ± 0.21
		Bloem	0.96 ± 0.30	0.74 ± 0.13	0.75 ± 0.17	0.95 ± 0.23
		Joburg/PTA	0.94 ± 0.29	0.76 ± 0.13	0.75 ± 0.15	0.97 ± 0.24
		HVAPA	0.98 ± 0.29	0.73 ± 0.13	0.75 ± 0.18	0.95 ± 0.22
		Durban	1.01 ± 0.27	0.72 ± 0.11	0.80 ± 0.20	0.95 ± 0.24
	South Africa	Average	1.00 ± 0.29	0.74 ± 0.12	0.76 ± 0.17	0.95 ± 0.22

Discussion Paper | Discussion Paper | Discussion Paper | Discussion Paper |

ACPD

14, 24701–24752, 2014

South African aerosol

S. P. Hersey et al.

Title Page

Abstract · Introduction

Conclusions · References

Tables · Figures

|◄ · ►|

◄ · ►

Back · Close

Full Screen / Esc

Printer-friendly Version

Interactive Discussion

Table 3. Average diurnal and monthly values of PM_{10} and $PM_{2.5}$ measured at the ground, separated by site type. All concentrations in $\mu g\,m^{-3}$.

			Township	Urban/Suburban Residential	Industrial
PM_{10}	Diurnal	Max	408	130	162
		Min	14	8	7
	Monthly	Max	169	88	109
		Min	23	28	10
		Mean	70 ± 31	46 ± 16	39 ± 23
$PM_{2.5}$	Diurnal	Max	123		
		Min	12		
	Monthly	Max	72		
		Min	23		
		Mean	38 ± 12		
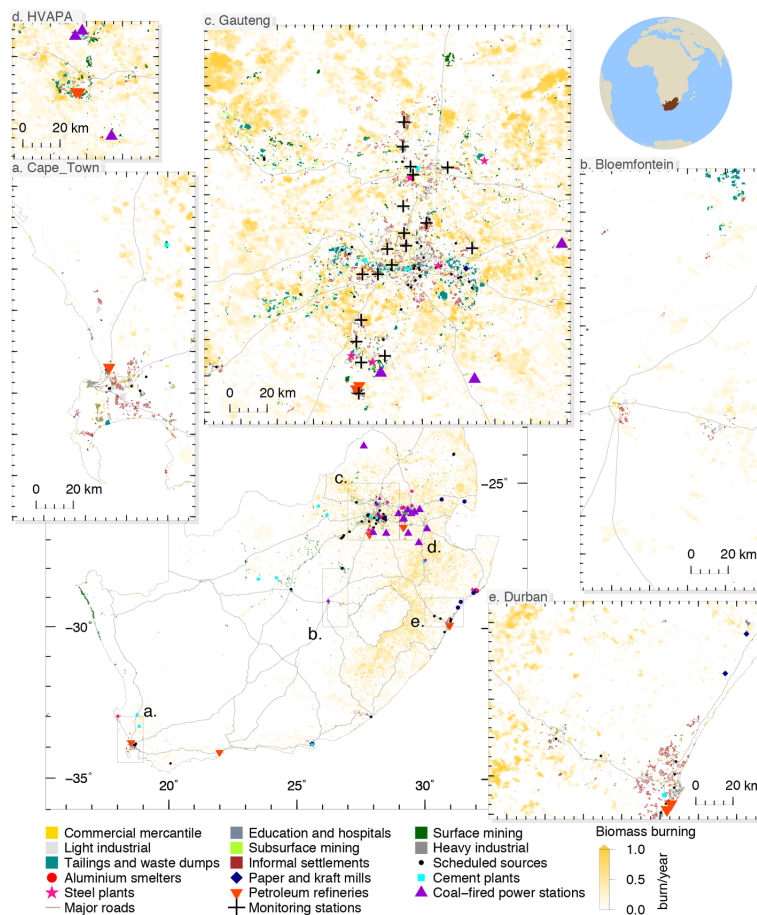
Figure 1. Map depicting satellite study grids, with a summary of area and point sources.
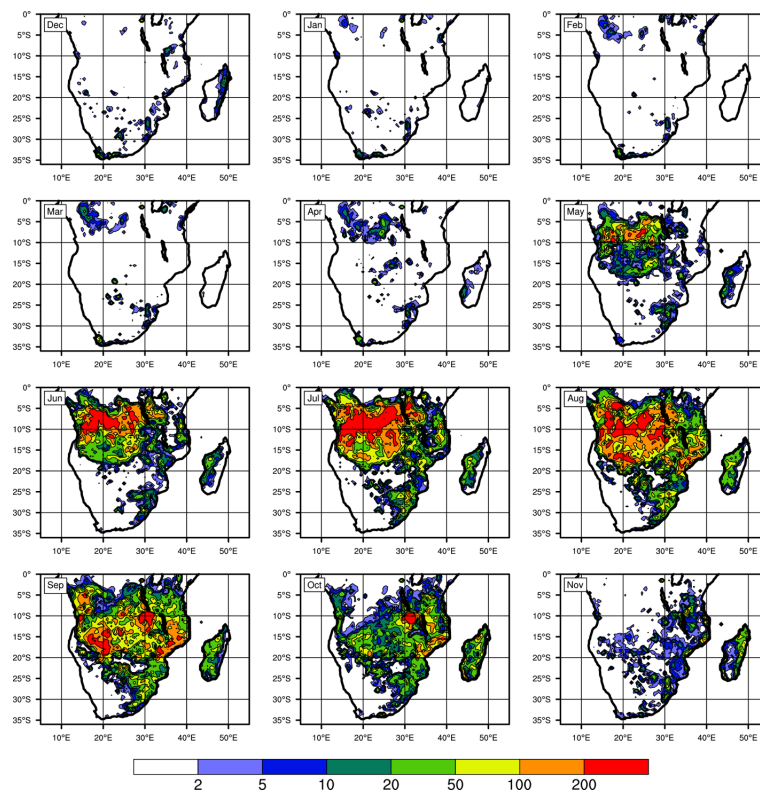
Figure 2. Monthly averaged FRP integrated over $0.5° \times 0.5°$ boxes in the Southern Africa Domain over the period 1 January 2000 to 31 December 2009 from MODIS thermal anomaly retrieval.

Full Screen / Esc

Printer-friendly Version

Interactive Discussion
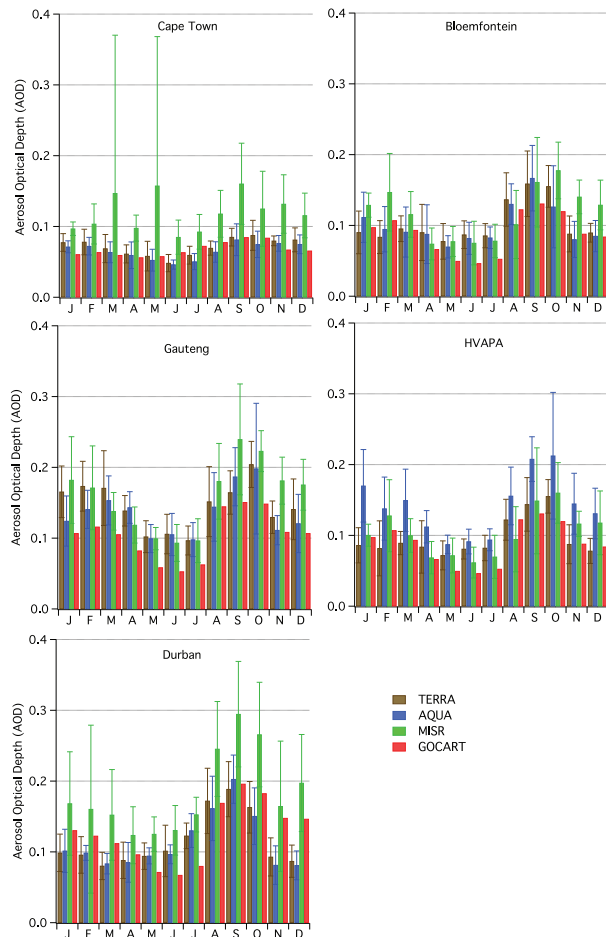
Figure 3. AOD averages for each region for the period 1 January 2000 to 31 December 2009. Error bars represent one standard deviation in the mean.

Title Page

Abstract   Introduction

Conclusions   References

Tables   Figures

|◄   ►|

◄   ►

Back   Close

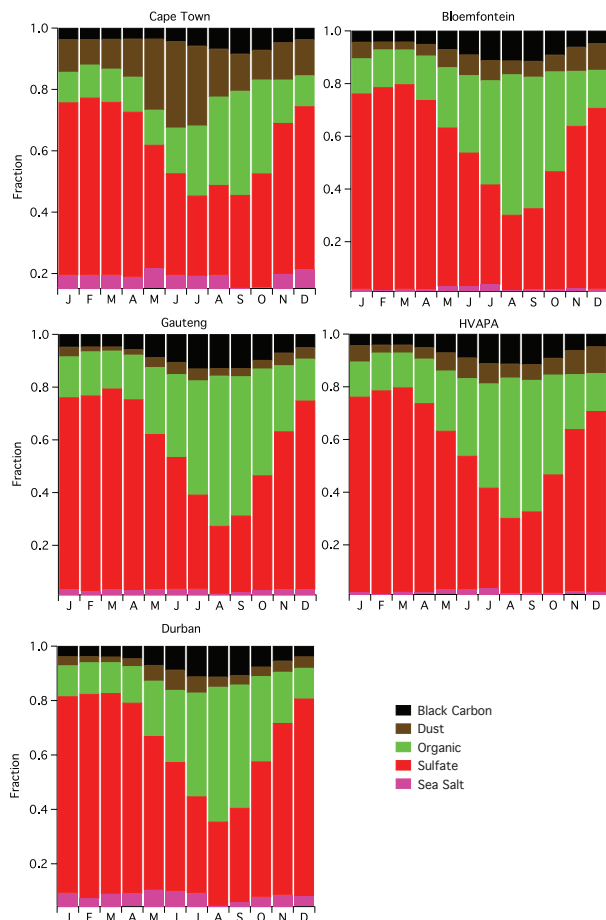Full Screen / Esc

Printer-friendly Version

Interactive Discussion
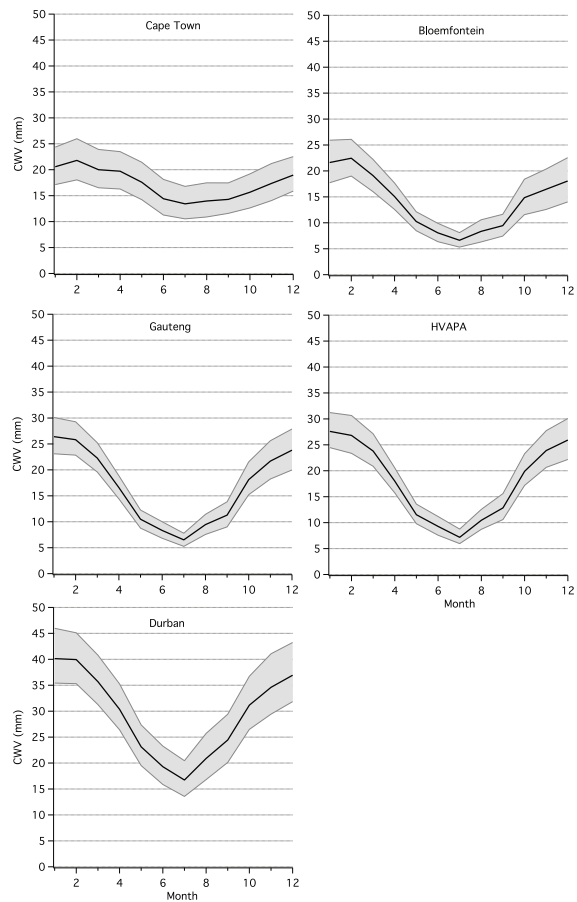
Figure 4. Average monthly column water vapor (CWV, black line) for the period 1 January 2000 to 31 December 2009, with gray shading representing minimum and maximum monthly CWV during that period.
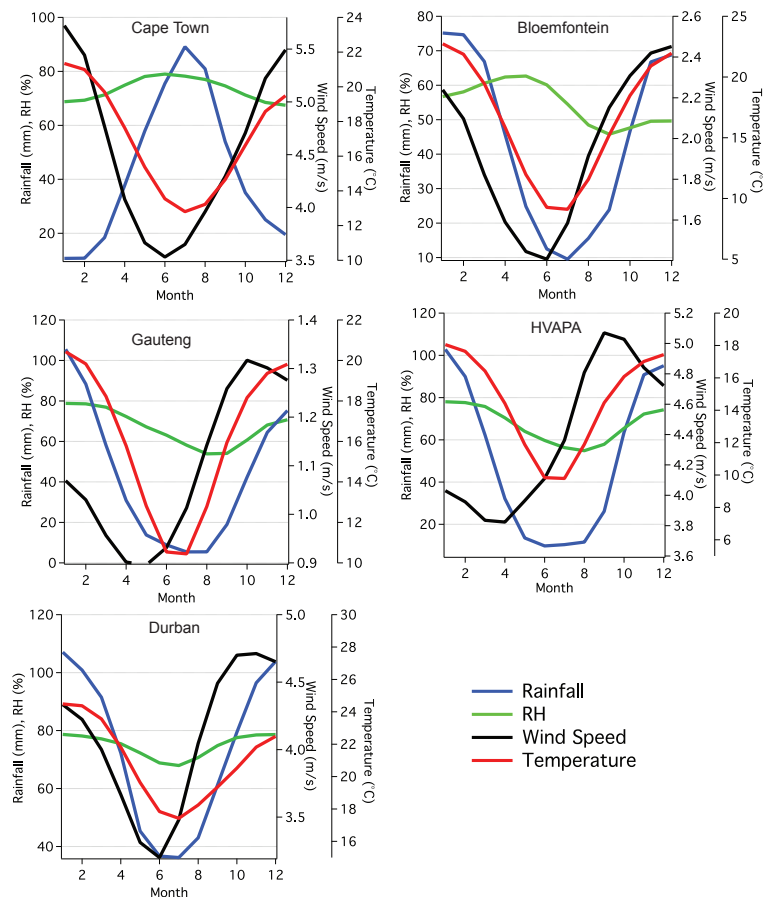
Figure 5. Monthly averaged values of RH, accumulated rainfall, wind speed, and temperature for sites in each satellite study area for the period 1 January 2000 to 31 December 2009. Note different *y* scales for each site.

Title Page

Abstract | Introduction

Conclusions | References

Tables | Figures

|◄ | ►|

◄ | ►

Back | Close

Full Screen / Esc

Printer-friendly Version

Interactive Discussion
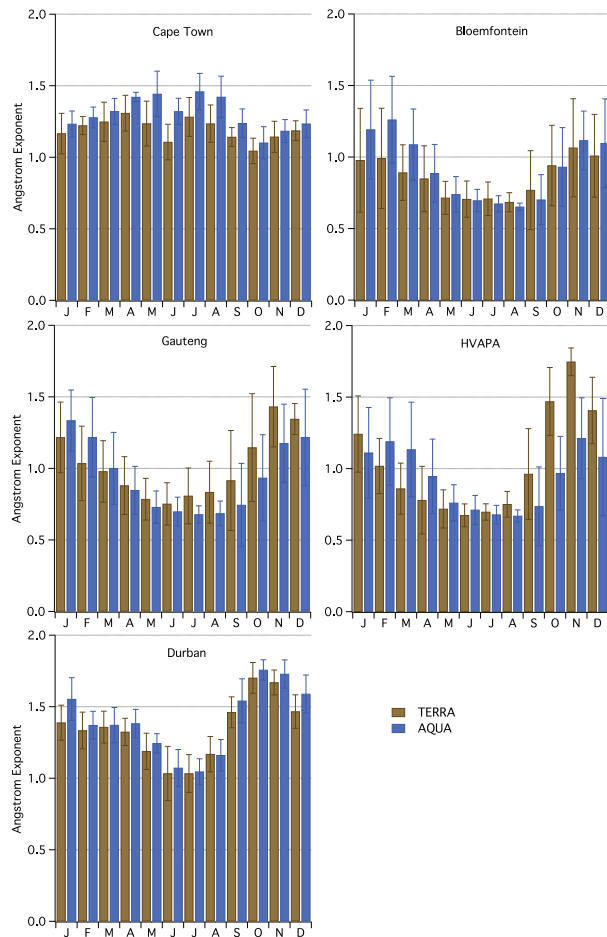
Figure 6. Monthly averaged values of Ängström Exponent (α) for each region for the period 1 January 2000 to 31 December 2009.

Figure 7. Monthly averaged values of UVAI for each region for the period 1 January 2000 to 31 December 2009.

Figure 8. Monthly averaged fractional contribution of various aerosol components to total AOD as modeled by GOCART. Data are presented for each region for the period 1 January 2000 to 31 December 2009.

Title Page

Abstract   Introduction

Conclusions   References

Tables   Figures

|◄   ►|

◄   ►

Back   Close

Full Screen / Esc

Printer-friendly Version

Interactive Discussion
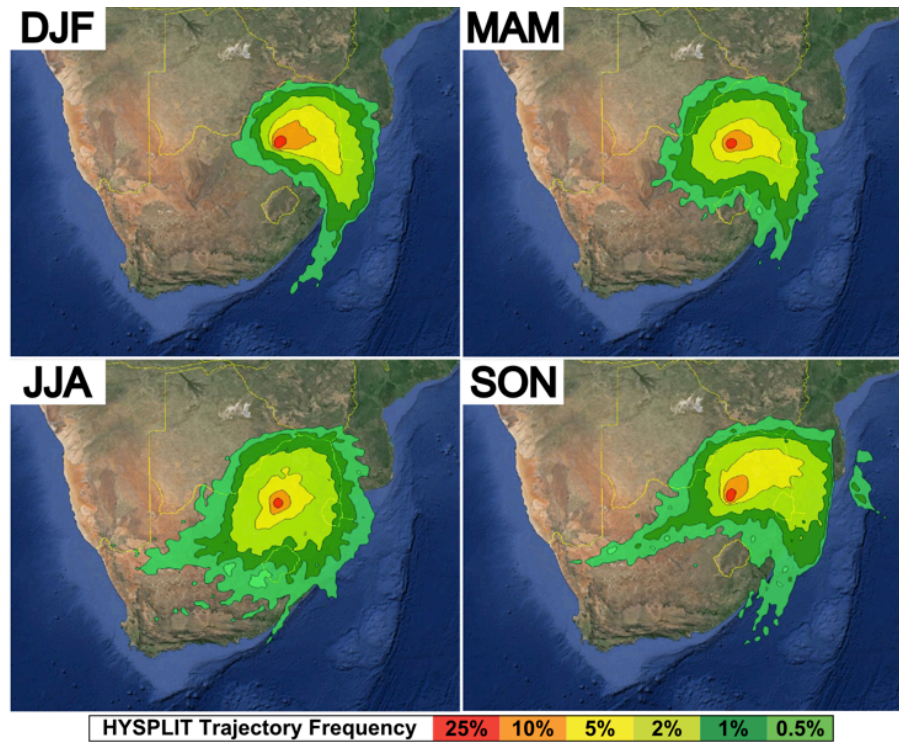
Figure 9. Frequency of airmass origin based on seasonal averages of 3 day HYSPLIT back-trajectories for Gauteng for the period 1 January 2000 to 31 December 2009.
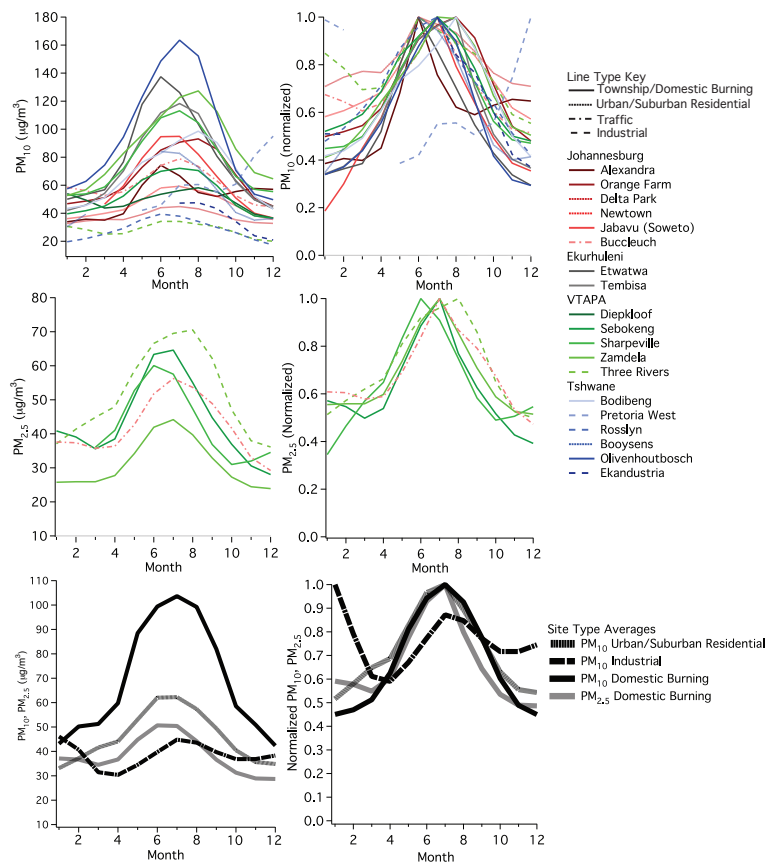
Figure 10. Monthly averaged PM_{10}, $PM_{2.5}$ (absolute magnitude and normalized by maximum monthly average) and $PM_{2.5}/PM_{10}$ for ground monitoring sites. Solid lines represent sites with domestic burning influence, fine dashed lines represent urban/suburban residential areas, and coarse dashed lines represent industrial sites.
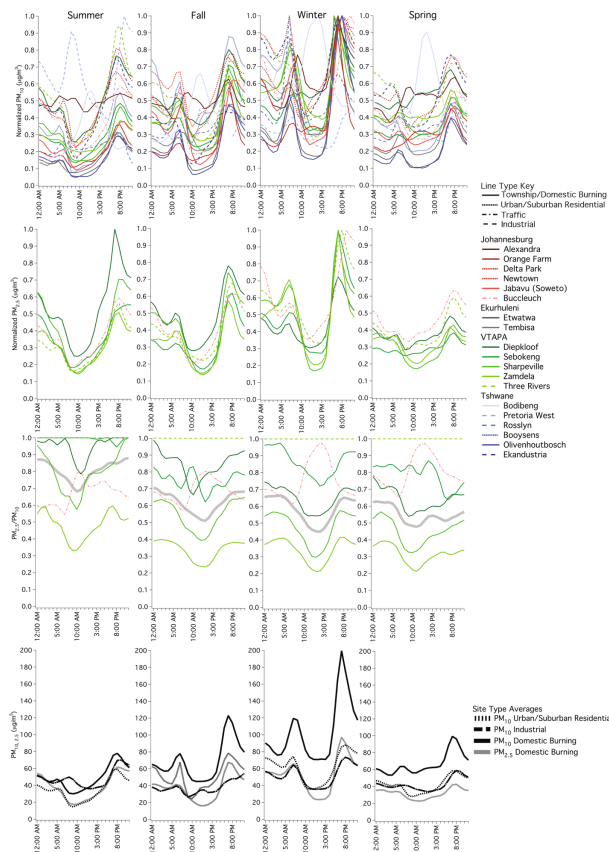
Figure 11. Season-averaged diurnal PM$_{10}$, PM$_{2.5}$, and PM$_{2.5}$/PM$_{10}$, with each site normalized by the maximum hourly average across all seasons. Solid lines represent sites with domestic burning influence, fine dashed lines represent urban/suburban residential areas, and coarse dashed lines represent industrial sites.
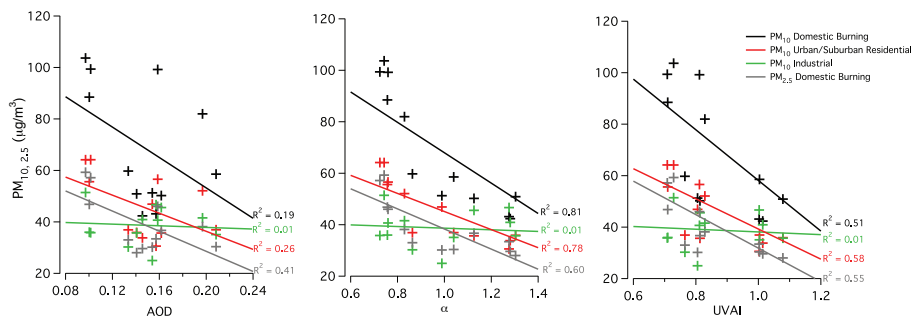
South African aerosol

S. P. Hersey et al.

Title Page

Abstract | Introduction

Conclusions | References

Tables | Figures

Back | Close

Full Screen / Esc

Printer-friendly Version

Interactive Discussion

Figure 12. Monthly averaged PM for each site type (domestic burning, urban/suburban residential, and industrial) plotted against monthly averaged satellite parameters (AOD, α, and UVAI). Linear least squares regression lines are plotted, with corresponding R^2 values listed for each fit.
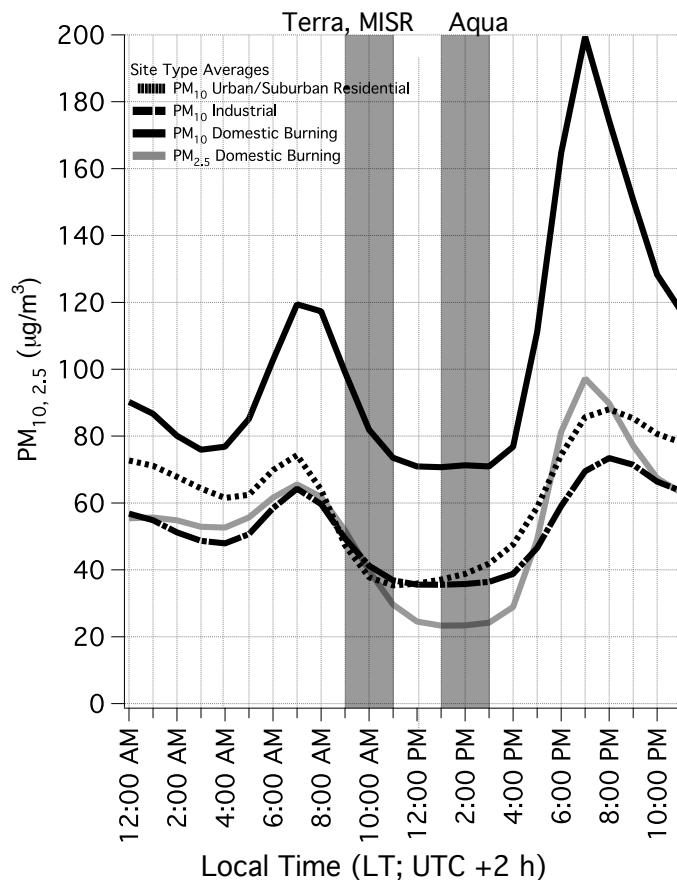
Figure 13. Winter diurnal ground PM_{10} and $PM_{2.5}$ concentrations, with shaded gray boxes representing satellite flyover times for Terra, Aqua, and MISR platforms.